Comparison of three stream tube models predicting field-scale solute transport

D. Jacques, J. Vanderborght, D. Mallants, D.-J. Kim, H. Vereecken, J. Feyen

Hydrology and Earth System Sciences, 4, 873–893 (1997) © EGS

Hydrology & Earth System Sciences

Comparison of three stream tube models predicting field-scale solute transport

Diederik Jacques[1]*, Jan Vanderborght[1], Dirk Mallants[1], Dong-Ju Kim[3], Harry Vereecken[2], and Jan Feyen[1].

[1] Institute for Land and Water Management, Katholieke Universiteit Leuven, Vital Decosterstraat 102, B 3000 Leuven, Belgium
[2] Forschungszentrum, KFA, Erdöl und Geochemie, ICG4, Jülich D 5170, Germany
[3] Department of Environmental Geosphere Science, Faculty of Science and Engineering, Korea University, An Am Dong, Seong Buk Ku, Seoul, Republic of Korea
* Corresponding Author (e-mail: diederik.jacques@agr.kuleuven.ac.be)

Abstract

In this paper the relation between local- and field-scale solute transport parameters in an unsaturated soil profile is investigated. At two experimental sites, local-scale steady-state solute transport was measured in-situ using 120 horizontally installed TDR-probes at 5 depths. Local-scale solute transport parameters determined from BTCs were used to predict field-scale solute transport using stochastic stream tube models (STM). Local-scale solute transport was described by two transport models: (1) the convection-dispersion transport model (CDE), and (2) the stochastic convective lognormal transfer model (CLT). The parameters of the CDE-model were found to be lognormally distributed, whereas the parameters of the CLT model were normally distributed. Local-scale solute transport heterogeneity within the measurement volume of a TDR-probe was an important factor causing field-scale solute dispersion. The study of the horizontal scale-dependency revealed that the variability in the solute transport parameters contributes more to the field-scale dispersion at deeper depths than at depths near the surface. Three STMs were used to upscale the local transport parameters: (i) the stochastic piston flow STM-I assuming local piston flow transport, (ii) the convective-dispersive STM-II assuming local CDE transport, and (iii) the stochastic convective lognormal STM-III assuming local CLT. The STM-I considerably underpredicted the field-scale solute dispersion indicating that local-scale dispersion processes, which are captured within the measurement volume of the TDR-probe, are important to predict field-scale solute transport. STM-II and STM-III both described the field-scale breakthrough curves (BTC) accurately if depth dependent parameters were used. In addition, a reasonable description of the horizontal variance of the local BTCs was found. STM-III was (more) superior to STM-II if only one set of parameters from one depth is used to predict the field-scale solute BTCs at several depths. This indicates that the local-scale solute transport process, as measured with TDR in this study, is in agreement with the CLT-hypothesis.

Introduction

To asses the risk of contaminant leaching from hazardous waste sites, it is crucial to describe and predict the field-scale solute transport accurately. Several studies have shown that the field-scale mean breakthrough curve (BTC) in a heterogeneous porous medium can be described by the one-dimensional macroscopic convection-dispersion equation (CDE) (Roth *et al.*, 1991; Jacques *et al.*, 1997). The transport parameters pertaining to the macroscopic CDE are usually called effective transport parameters. These are the effective average solute particle velocity, v_{eff} [L T^{-1}], and the effective dispersion coefficient, D_{eff} [L^2 T^{-1}]. The effective parameters incorporate the complex tortuous flow path of the solutes as well as the horizontal and vertical heterogeneity of the soil (Beven *et al.*, 1993). Based on column-scale (e.g., Khan and Jury, 1990; Zhang, 1995; Mallants, 1996; Vanderborght *et al.*, 1997a) and field-scale solute transport studies (e.g., Butters and Jury, 1989; Jacques *et al.*, 1997), it was shown that D_{eff} increases with increasing transport distance. Consequently, field-scale solute transport can only be described by a 1-D CDE model by assigning different parameters to different depths. Furthermore, D_{eff} is larger than the local dispersion coefficient, D, due to horizontal variability of the local pore water velocity, v (Amoozegard-Fard *et al.*, 1982; Mallants *et al.*, 1996; Toride and Leij, 1996a,b).

As an alternative to the use of the classical CDE in describing field-scale solute transport, Jury *et al.* (1982)

proposed a transfer function approach. This approach relates the output variable of interest (e.g., field-scale BTC at a given depth) to an input condition (e.g., a finite pulse input). One model is the stochastic convective lognormal transfer function model (CLT, Jury, 1982) which assumes that the velocity of a solute particle remains constant along its travel path through the soil. Furthermore, the probability density function (pdf) of solute particle velocities is assumed to be lognormally distributed. This model has been used successfully in several studies to describe the mean field-scale transport process (e.g., Jury *et al.*, 1982; Butter and Jury, 1989; Jacques *et al.*, 1997).

In the last decade, several models became available for the prediction of the field-scale BTC and the corresponding effective parameters from the statistical moments of local soil hydraulic properties. Apart from the stochastic models which describe 2-D and 3-D solute transport in heterogeneous soils (e.g., Russo, 1993; Tseng and Jury, 1994; Roth and Hammel, 1996; Harter and Yeh, 1996; Vanderborght *et al.*, 1997b), there is a set of models referred to as stream tube models (STM) which assumes 1-D water flow and solute transport (Dagan and Bresler, 1979 and Bresler and Dagan, 1979). In this model, solute flow is coupled to the water flow equation and solved for heterogeneous velocity fields determined by the statistics of the soil hydraulic properties. Recently, Dagan (1993) and Destouni (1993) extended these STMs for reactive transport and solute transport in macroporous and layered soils.

Another group of STMs predicts field-scale transport in heterogeneous soils based on local-scale observations of solute transport instead of observations of local soil hydraulic properties. Several different types of such STMs have been developed. They are distinguished by conceptual differences in the description of local transport such as local piston flow (Jury and Roth, 1990); local convection-dispersion transport process (Toride and Leij, 1996a,b); or local stochastic convective solute transport (Vanderborght *et al.*, 1997a). The objective of these models is to upscale local-scale parameters for describing field-scale BTCs and to derive values of D_{eff} at different depths to predict BTCs throughout the soil profile. However, studies of the validation of these different STM using field-scale observations or comparison of different local-scale transport models are rare in the present literature.

The main objective of the present study is to compare the predictive capacities of 3 STMs. For this purpose, solute transport was measured at two sites along a transect of 8 m (5 depths and 24 locations) using horizontally installed TDR-probes. Statistical analysis of the measured transport behaviour at the local scale provides an estimate of the field-scale transport, in addition to the input data necessary for the stream tube models. Jacques *et al.* (1997) described the experimental design and identified the governing transport processes at the field-scale using the field-averaged BTC. In this paper, the statistical parameters describing the variability of the local-scale BTCs are determined and the three STMs are compared. In a theoretical section, the mathematical concepts of the three STMs are reviewed briefly and it is shown how they relate the pdf of local-scale transport parameters to the field-scale transport. The field experiments are then described and the methods used to identify (a) the multivariate pdf of the local-scale transport parameters, and (b) the horizontal scale-dependency of the solute parameters are discussed.

Theory of Stream Tube Models

The field-scale solute transport process is restricted to 1-D solute transport and solute particles are moving vertically downwards in stream tubes without exchange of water and solutes between the stream tubes (Fig. 1, top figures). Stream tubes with a high average solute particle velocity at time $t = 0$ also have a high average solute particle velocity at time $t = t + \Delta t$. Therefore, the field-scale solute travel time variance and D_{eff} increase with depth. Although this is not a universal trend in solute transport through the unsaturated zone, it was observed in many field-scale solute transport experiments (e.g., Butters and Jury, 1989; Hamlen and Kachanoski, 1992; Ellsworth *et al.*, 1996; Rudolph *et al.*, 1996).

The solute transport at the local-scale, i.e., within a single stream tube, can be described as either (i) a piston flow type process which neglects intra-scale heterogeneity (i.e., absence of local-scale dispersion, Fig. 1a), (ii) a convection-dispersion process (Fig. 1b), or (iii) a stochastic convective process (Fig. 1c). Both the convection-dispersion and the stochastic convective model include intra-scale heterogeneity. The local-scale parameters of these three models are considered spatially variable and are treated mathematically as spatially uncorrelated random variables, X. The multivariate pdf, $f_X(x_1, \ldots, x_n)$ where $x_1, \ldots, x_n$ are the parameters describing the local-scale process model of choice (i, ii, or iii), is determined from field experiments, in which a large number of local BTCs are measured. Thus a (random) sample of local-scale transport parameters X is obtained by matching the local-scale process model to the locally measured BTCs. Assuming stationarity and ergodicity, the sample pdf obtained from a single realization can be considered representative for the multivariate pdf $f_X(x_1, \ldots, x_n)$. Once $f_X(x_1, \ldots, x_n)$ is known, the STM model allows prediction of the field-scale solute concentration, which is defined as the ensemble mean concentration, $\langle C(z,t) \rangle$, at depth z, given a time t. Brackets ($\langle \rangle$) indicate the expectation operator. The ensemble mean is computed by integration (Jury and Roth, 1990, eq. 4.1):

$$\langle C(z,t) \rangle = \int_{-\infty}^{+\infty} \cdots \int_{-\infty}^{+\infty} C(z,t;x_1,x_2,\ldots,x_n) f_X(x_1,x_2,\ldots,x_n) dx_1 dx_2 \ldots dx_n \quad (1)$$

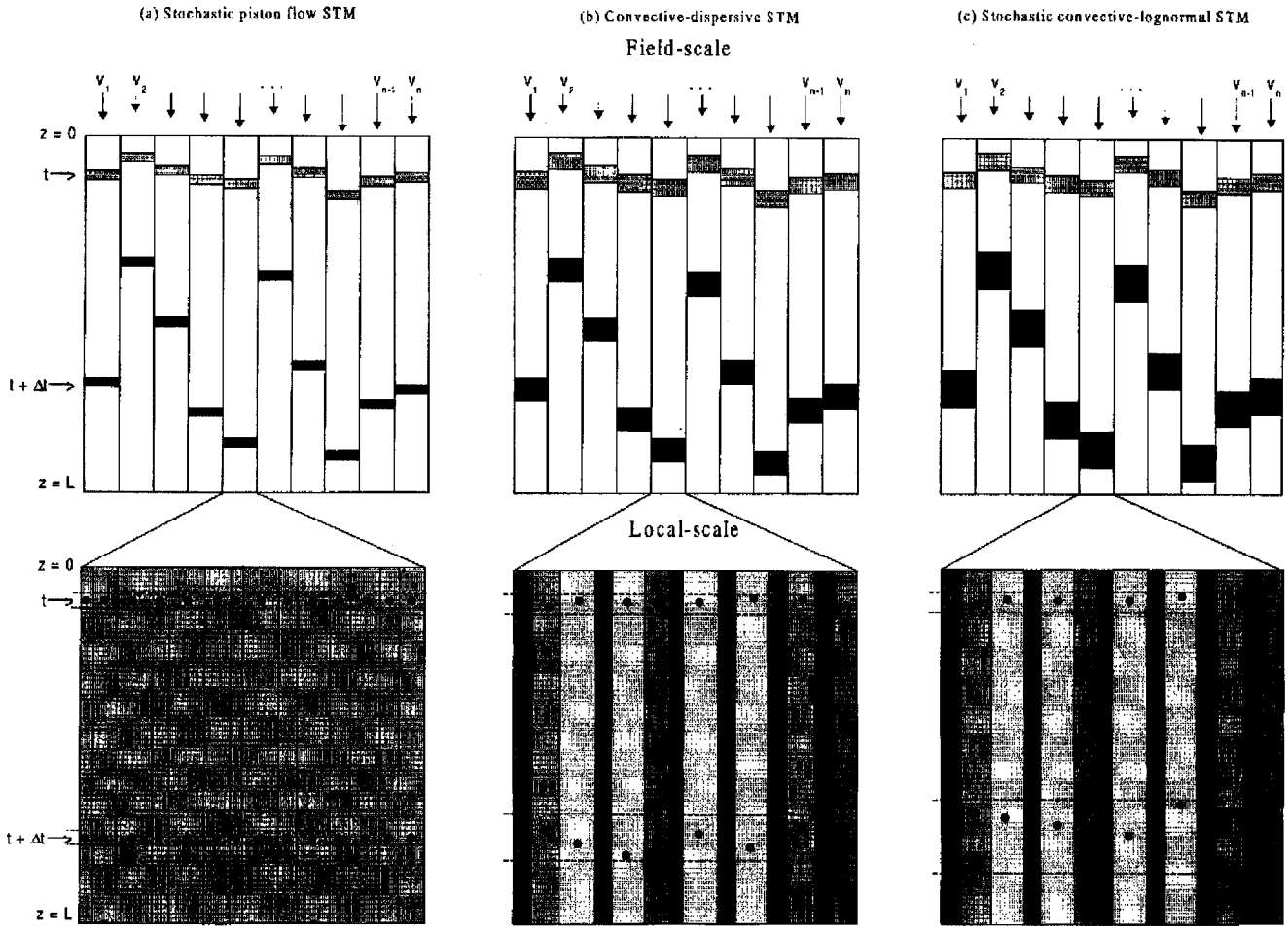

Fig. 1. *Schematic representation of the three stream tube models at the field-scale (top) and the local-scale (bottom) for (a) the stochastic piston flow model, (b) the convective-dispersive STM and (c) the stochastic convective-lognormal STM. For the field-scale, light shaded and dark shaded areas illustrate solute distribution in the stream tubes at time t and t+Δt after a pulse application of constant duration, respectively. For the local-scale, solute particle variance is indicated with the dashed line at time t and t + Δt.*

where $C(z,t;x_1,x_2,\ldots,x_n)$ is the solute concentration at depth z and time t in the stream tube, $x_1,x_2,\ldots,x_n$ are the transport parameters within each stream tube, and $f_X(x_1,x_2,\ldots,x_n)$ is the joint multivariate pdf of the solute transport parameters (e.g., the bivariate normal or lognormal pdf (Eqn. 14)). Variability in local BTCs leads to field-scale dispersion that is larger than local-scale dispersion. Field-scale dispersion is the combined effect of local-scale dispersive processes (due to heterogeneity within a stream tube) and the field-scale variability of local scale BTCs, expressed by the variance of $C(z,t)$, $Var[C(z,t)]$. The variance of the local BTCs at depth z is given as (Jury and Roth, 1990):

$$Var\left[C(z,t)\right] = \int_{-\infty}^{+\infty} \cdots \int_{-\infty}^{+\infty} \left[C(z,t;x_1,x_2,\ldots,x_n) - \left\langle C(z,t)\right\rangle\right]^2 f_X(x_1,x_2,\ldots,x_n)dx_1dx_2\ldots dx_n \quad (2)$$

Solute concentrations can be represented as flux-averaged concentrations, $C^f(z,t)$, or as resident or volume-averaged concentrations, $C^r(z,t)$. The latter concentration mode is of particular interest in this study because solute concentrations were obtained using TDR (see next section). Since the local-scale concentration mode is also of this type, both the local- and field-scale models will be expressed as time normalized resident concentrations. For each of the three different conceptual STMs, the following sections will briefly introduce (a) the local-scale transport model and the approach used to obtain local-scale parameters from measured local-scale BTCs, and (b) the effective parameters describing field-scale mean transport defined by Eqn. (6). For the latter it is assumed that field-scale solute transport (Eqn. 6) follows the standard convection-dispersion equation.

STOCHASTIC PISTON FLOW STM

The first model assumes that local solute flow can be described by a piston flow process resulting in the field-scale *stochastic piston flow model* (Fig. 1a). All solute parti-

cles in a single stream tube have the same velocity. At the local scale, there is no solute dispersion and the solute spreading does not increase with depth (Fig. 1a, bottom). However, the pore water velocity differs between the different stream tubes causing the field-scale solute dispersion. Many studies have shown that the different convection velocities are caused by the spatial variability in the soil hydraulic properties (e.g., Biggar and Nielsen, 1976; Bowman and Rice, 1986; Destouni *et al.*, 1994).

For a narrow pulse of solute at the surface (a Dirac-delta input function), the field-scale time-normalized flux concentration at a depth z is equal to the field-scale solute travel time pdf, $f^f(z,t)$, which can be related to the pdf of the solute particle velocities, $f_V(v)$, as (Jury and Roth, 1990, Eqn. 4.4):

$$\frac{C^f(z,t)}{\int_0^\infty C^r(z,t)dt} \equiv f^f(z,t) = \frac{z}{t^2} f_V(v) \tag{3}$$

For stream tube transport, the field-scale time-normalized resident concentrations, $<C^{rt^*}(z,t)>$ can be written in terms of $f^f(z,t)$ as (Vanderborght *et al.*, 1996):

$$\left\langle \frac{C^r(z,t)}{\int_0^\infty C^r(z,t)dt} \right\rangle = \left\langle C^{rt^*}(z,t) \right\rangle = \frac{t f^f(z,t)}{T_1^f} = \frac{z}{t}\frac{f_V(v)}{T_1^f} = v\frac{f_V(v)}{T_1^f} \tag{4}$$

where T_1^f is the first time moment of the travel time flux pdf. If the distribution of the average solute particle velocities is specified, T_1^f can be calculated as $T_1^f = E_z(t) = z\,E_V(1/v)$ where $E_V(.)$ is the expectation or ensemble average of $f_V(v)$. If it is assumed that $f_V(v)$ is a lognormal pdf, then T_1^f is given as:

$$T_1^f = z\exp(-\mu_{lnv} + 0.5\sigma_{lnv}^2) \tag{5}$$

where μ_{lnv} and σ_{lnv} are the mean and the standard deviation of the $\log_e$-transform of v obtained from the locally measured BTCs.

If the field-scale solute transport can be described by a convection-dispersion equation with effective transport parameters:

$$\frac{\partial\langle C^{rt^*}\rangle}{\partial t} = D_{eff}\frac{\partial^2\langle C^{rt^*}\rangle}{\partial z^2} - v_{eff}\frac{\partial\langle C^{rt^*}\rangle}{\partial x} \tag{6}$$

with the effective parameters v_{eff} and D_{eff}. The effective parameters can be expressed as a function of the statistical moments of the local-scale transport parameters (Table 1). For the piston-flow model, the first and second travel time moment of the field-scale solute flux BTC (Eqn. 3) are expressed as a function of μ_{lnv} and σ_{lnv}. For the specified boundary conditions in this study, these travel time moments can be related to the effective parameters v_{eff} and D_{eff} of Eqn. (6) (Leij and Dane, 1991) resulting in the expressions in Table 1.

Table 1. Effective parameters of the macroscopic CDE as a function of the statistics of the local-scale solute transport parameters.

	v_{eff}	D_{eff}
PF – STM *	$\exp(-\mu_{lnv} + 0.5\sigma_{lnv}^2)^{-1}$	$\frac{z}{2}\frac{(\exp(\sigma_{lnv}^2)-1)}{\exp(-\mu_{lnv}+0.5\sigma_{lnv}^2)}$
CD – STM	$z\left[\frac{2\langle D\rangle}{\langle v\rangle^2}\exp(3\sigma_v^2 - 2\rho_{vD}\sigma_v\sigma_D) + \frac{2z}{\langle v\rangle}\exp(\sigma_v^2) - \left[\frac{4\langle D\rangle^2}{\langle V\rangle^4}\exp(10\sigma_v^2 - 8\rho_{vD}\sigma_v\sigma_D + \sigma_D^2) + \frac{4\langle D\rangle z}{\langle v\rangle^3}\exp(6\sigma_v^2 - 3\rho_{vD}\sigma_v\sigma_D) + \frac{z^2}{\langle v\rangle^2}\exp(3\sigma_v^2)^{0.5^{-1}}\right]\right]$	$z^2\left[\left[\frac{4\langle D\rangle^2}{\langle V\rangle^4}\exp(10\sigma_v^2 - 8\rho_{vD}\sigma_v\sigma_D + \sigma_D^2) + \frac{4\langle D\rangle}{\langle v\rangle^3}\exp(6\sigma_v^2 - 3\rho_{vD}\sigma_v\sigma_D) + \frac{z^2}{\langle v\rangle^2}\exp(3\sigma_v^2)\right]^{0.5} - \left[\frac{\langle D\rangle z}{\langle v\rangle^2}\exp(3\sigma_v^2 - 2\rho_{vD}\sigma_v\sigma_D) + \frac{z}{\langle v\rangle}\exp(\sigma_v^2)\right]\right]$
SC – STM	$\langle v\rangle$	$0.5z\langle v\rangle[\exp(\sigma_{lnv} + \langle\sigma\rangle^2) - 1]$

* Stochastic piston flow STM

CONVECTIVE-DISPERSIVE STM

In the second model, it is assumed that local-scale solute transport can be described as a convection-dispersion process (CDE) and the field-scale model is referred to as a *convective-dispersive STM* (CD-STM, Toride and Leij, 1996a,b) (Fig. 1b). The CDE-model represents an infinite time process by assuming that the time for mixing is small compared to the convection time (Jury and Flühler, 1992). Within a single stream tube, pore groups with different pore water velocities are present and solute particles mix between the different pore groups. Consequently, the solute particle arrival time at depth $z = z_1$ is uncorrelated with the solute arrival time at $z = z_2$ and the solute arrival time variance increases linearly with depth (Fig. 1b, bottom). The field-scale dispersion is the result of both the local-scale dispersion and the horizontal variability of the local-scale CDE-transport parameters. Toride and Leij (1996a,b) investigated theoretically the influence of the statistics of the local-scale parameters on the field-scale BTC, the variance, v_{eff} and D_{eff}. Previous tests of the applicability of the CD-STM were based on a numerical experiment (Toride and Leij, 1996b) and a lysimeter-study (Mallants, 1996).

The analytical solution of the local-scale CDE model for a mobile, conservative, inert solute applied as a narrow pulse at the soil surface (Boundary Value Problem) is (Jury and Roth, 1990, eqn. 3.12):

$$C^{rt^*}(z,x,t) = \frac{v}{\sqrt{\pi D t}} \exp\left[-\frac{(z-vt)^2}{4Dt}\right] - \frac{v^2}{2D}\exp\left[\frac{vz}{D}\right] erfc\left[\frac{z+vt}{\sqrt{4Dt}}\right] \quad (7)$$

where v is the average solute particle velocity [cm day^{-1}] and D is the dispersion coefficient [cm^2 day^{-1}]. The local-scale parameters v and D are obtained here by fitting Eqn. (7) to the measured BTCs using the SAS NLIN-procedure (SAS Institute Inc., 1989).

The field-scale solute concentration is obtained by replacing $C(z,t;x_1,x_2,\ldots,x_n)$ in Eqn. (1) by the time-integrated normalized resident concentration (Eqn. (7)). Toride and Leij (1996a) further assumed (i) that the random parameters v and D can be described with a bivariate lognormal distribution and (ii) that the soil water content, θ, is deterministic over all stream tubes so that local differences in v are caused entirely by the variability in water flux density. This simplification is justified because the coefficient of variation, CV, of θ is sufficiently small, generally 0.2 or less (Jury, 1985). Since water was applied uniformly at the input surface of the two experimental fields, water is assumed to be funnelled due to horizontal redistribution close to the input surface.

The field-effective parameters v_{eff} and D_{eff} of Eqn. (6) are derived from the time moments of the field-scale resident BTC. These time moments were expressed as a function of $<v>$, $<D>$, σ_v, σ_D, and ρ_{vD} with $<v>$ and $<D>$ the ensemble averages of v and D (see Eqn. 19), σ the standard deviation of log-transformed variables and ρ_{vD} the correlation coefficient (see Eqn. 17). These expressions are derived using Eqn. (A3) in Toride and Leij (1996a). The resulting expressions are given in Table 1.

STOCHASTIC CONVECTIVE LOGNORMAL STM

The third model considers a local stochastic convection solute transport process (Simmons, 1982). The solute particles have different velocities as is the case in the local CDE-model, but the velocity of a solute particle does not change with depth. The different solute particle velocities originate from different pore water velocities within a single stream tube. In contrast with the CDE-model, however, there is no exchange of solute particles between pores with different water velocities. Solute particle arrival times are perfectly correlated and the solute arrival time variance increases quadratically with depth (Fig. 1c, bottom). In this study, the convective lognormal transfer function model (CLT, Jury, 1982) is used which assumes a lognormal pdf of the pore water velocities. The field-scale model is called a *stochastic convective lognormal STM* (SC-STM, Fig. 1c). Vanderborght *et al.* (1996a) expressed the field-scale parameters as a function of the statistics of the local-scale CLT parameters. However, they could not validate the expressions since there was no representative observed field-scale transport available.

For a narrow pulse of a conservative solute at the soil surface, $C^{rt^*}(z,x,t)$ is described by the CLT- model as (Vanderborght *et al.*, 1996):

$$C^{rt^*}(z,x,t) = \frac{l}{z}\frac{1}{\sigma_l\sqrt{2\pi}} \exp\left[-\frac{\left(\ln\left(\frac{tl}{z}\right)-\mu_l\right)^2}{2\sigma_l^2} - \mu_l - \frac{\sigma_l^2}{2}\right] \quad (8)$$

with μ_l and σ_l the CLT-parameters and l is the reference depth, defined since μ_l is dependent on the depth of calibration. Therefore, each BTC is transformed to the reference depth (in this study, the reference depth is 100 cm) by Eqn. (2.65) in Jury and Roth (1990). The parameters μ_l and σ_l are obtained by fitting Eqn. (8) to the observed local-scale BTC using the SAS NLIN-procedure (SAS Institute Inc., 1989). The average solute particle velocity v and the dispersion coefficient D, assuming a CLT-transport process, can be calculated from μ_l and σ_l as follows (Jury and Sposito, 1985):

$$v_{CLT} = l\exp(-\mu - 0.5\sigma^2) \quad (9)$$

$$D_{CLT} = \frac{zl}{2}\frac{(\exp(\sigma^2)-1)}{\exp(\mu+0.5\sigma^2)} \quad (10)$$

Assuming that the field-scale transport process can be represented by a field-scale CLT-model (Eqn. 8) and that $f_V(v)$ is a lognormal pdf, the field-scale solute BTC with effective parameters μ_{eff} and σ_{eff} can be written as a function of the local solute transport parameters (Vanderborght *et al.*, 1997a):

$$\mu_{eff} = \ln(z/\langle v\rangle) - \tfrac{1}{2}\sigma^2_{lnv} - \tfrac{1}{2}\langle\sigma\rangle^2 \quad (11)$$

$$\sigma^2_{eff} = \sigma^2_{lnv} + \langle\sigma\rangle^2 \quad (12)$$

where v is expressed as a function of the local-scale CLT-model parameters (Eqn. 9), $\sigma_{\ln v}$ is the standard deviation of the $\log_e$-transformed v, $<v> = \exp(\mu_{\ln v} + 0.5\sigma^2_{\ln v})$ with $\mu_{\ln v}$ the mean of the $\log_e$-transformed v and $<\sigma>$ is the ensemble average of the local model parameter σ. Assuming that the variability of θ and σ is small compared to the variability of v, θ and σ are treated as deterministic over all sets of sampled stream tubes. Field-scale transport may be conceptualized as the response of an injected solute pulse subject to several sources of spatial variability, one arising from the variability in solute velocity v within a set of stream tubes (characterized by σ) and one from the variability in solute velocity v between different sets of stream tubes. Using Eqns (11) and (12) in Eqns (9) and (10), the effective parameters v_{eff} and D_{eff} are obtained (Table 1).

Materials and Methods

DESCRIPTION OF THE FIELD EXPERIMENT

Two field experiments were conducted to monitor the solute plume movement in an undisturbed field plot under steady-state conditions for a loamy and a silty-loam soil. The loamy soil is located in an orchard at Bekkevoort (Belgium) and is classified as an Eutric Regosol in the FAO-classification system. The soil profile consists of three main horizons, i.e., Ap (0–25 cm), C1 (25–55 cm), and C2 (55–100 cm) with an abundance of mainly vertically oriented macropores throughout the soil profile (Mallants *et al.*, 1997a). The silty-loam soil is located in a fallow soil at Jülich (Germany) and has five distinct horizons: Ap (0–30 cm), Eg (30–40 cm), Btg1 (40–60 cm), Btg2 (60–100 cm) and C (> 100 cm). In the FAO-classification system, it is classified as a Stagnic Podzoluvisol. A detailed description of the experimental design, TDR-calibration and identification of the transport process at the field-scale is given by Jacques *et al.* (1996). However, for the benefit of the reader, a short description of the experimental procedure will be repeated here.

In an 8 m long and 1 m deep trench, triple-wire TDR-probes were installed horizontally at 24 locations and 5 depths at each location. In Bekkevoort, measuring depths were at 10, 30, 50, 70 and 90 cm and the horizontal spacing was 35 cm. At Jülich, TDR-probes were installed at 15, 35, 50, 70 and 90 cm depth with a horizontal spacing of 33 cm. An irrigation system applied a constant water flux of 2.8 cm day^{-1} in Bekkevoort and 1.5 cm day^{-1} in Jülich. After three weeks of irrigation, steady-state flow conditions were established. A pulse of $CaCl_2.2H_2O$ with a concentration of 87.5 g l^{-1} and 80 g l^{-1} was applied during 5.7 and 8 hours for Bekkevoort and Jülich, respectively, so that the water flux during solute application was identical to the steady-state water flux. After solute application, the irrigation was restarted and the downward leaching of the solute plume was monitored with an automated TDR-system developed by Heimovaara and de Water (1993). Measurements of the soil water content and bulk electrical conductivity were taken every 2 hours in Bekkevoort and every 4 hours in Jülich over a period of 42 and 65 days for Bekkevoort and Jülich, respectively.

DETERMINATION OF LOCAL-SCALE BTCS

The TDR measured resistance to flow of an electromagnetic wave through soil, R [Ω], was corrected for cable resistance and temperature and converted to the bulk soil electrical conductivity, EC_a [dS m^{-1}], following the method of Heimovaara and de Water (1993). EC_a was transformed to the electrical conductivity of the soil water, EC_w [dS m^{-1}], using the three-pathway conductance model of Rhoades *et al.* (1989). Finally, EC_w was converted to total resident concentration C^r (g l^{-1}) using an empirical relation. The calibration method invoked gave mass recoveries for the mean breakthrough curves ranging from 88% to 164% for the Bekkevoort and 102% to 118% for the Jülich field site (Jacques *et al.*, 1996).

The local-scale solute transport is measured with TDR-probes sampling an average soil volume of approximately 5000 cm^3. The measured resident concentrations, $C^r(z,x,t)$ at depth z [cm], location x [cm], and time t [day] were transformed to time-integrated normalized resident concentrations, $C^{r\,t^*}(z,x,t)$ [day^{-1}]:

$$C^{rt^*}(z,x,t) = \frac{C^r(z,x,t)}{\int_0^\infty C^r(z,x,t)dt} \quad (13)$$

FIELD-AVERAGED TRANSPORT

The field-scale BTCs were calculated as the arithmetic averages of the local BTCs across the horizontal plane. Field-scale BTCs for all 5 depths were analysed in terms of average solute arrival time, $E_z(t)$, and travel time variance, $Var_z(t)$. In Bekkevoort, solute transport was highly influenced by the presence of macropores, as was previously shown by Mallants *et al.* (1994, 1996). The observed solute movement was slower near the soil surface then at greater depths since more macropores were present at the shallow depth (Mallants *et al.*, 1997b), resulting in a larger amount of water bypassing the TDR sampling volume. Jacques *et al.* (1996) found an increase of the dispersivity,

λ [cm], for both soils except at the fifth depth in field Jülich. A maximum of 6.4 cm was measured at 90 cm depth for Bekkevoort and 7.3 at 70 cm depth for Jülich. The field-scale solute transport behaviour was better described by a stochastic convective process than by a convection dispersion process.

IDENTIFICATION OF MULTIVARIATE PROBABILITY DENSITY FUNCTION

Prediction of field-scale solute transport using one of the three STM models requires the multivariate pdf of the local-scale parameters. Two multivariate pdfs will be considered in this study: (i) the bivariate normal and (ii) the bivariate lognormal pdf, given by (Spiegel, 1992):

$$f(x,y) = \frac{1}{2\pi\sqrt{1-\rho_{xy}^2}} \exp\left[-\frac{Y_x^2 - 2\rho_{xy}Y_xY_y + Y_y^2}{2(1-\rho_{xy}^2)}\right] dY_x dY_y \tag{14}$$

with

$$Y_x = \frac{x-\mu_x}{\sigma_x}, \quad Y_y = \frac{y-\mu_y}{\sigma_y} \tag{15}$$

where $\mu_.$ and $\sigma_.$ are the mean and standard deviation of the untransformed variables for the case of the bivariate normal distribution. For the case of the bivariate lognormal pdf, expression of Y_x and Y_y are:

$$Y_x = \frac{\log_e(x) - \mu_{lnx}}{\sigma_{lnx}}, \quad Y_y = \frac{\log_e(y) - \mu_{lny}}{\sigma_{lny}} \tag{16}$$

with $\mu_{ln.}$ and $\sigma_{ln.}$ the mean and standard deviation of the $\log_e$-transformed variables. The correlation coefficient, ρ_{xy}, between Y_x and Y_y is given by

$$\rho_{xy} = \langle Y_xY_y \rangle = \int_{-\infty}^{+\infty}\int_{-\infty}^{+\infty} Y_xY_y f(x,y)dxdy \tag{17}$$

where x,y are v, D for the CDE and μ_l, σ_l for the CLT, respectively. The ensemble average of a parameter, <x>, and the coefficient of variation (CV) are given by (Aitcheson and Brown, 1963):

$$\langle x \rangle = \mu_x$$
$$CV = \sigma_x / \mu_x \tag{18}$$

for the normal pdf and:

$$\langle x \rangle = \exp(\mu_{lnx} + 0.5\sigma_{lnx}^2)$$
$$CV = (\exp(\sigma_{lnx}^2) - 1)^{0.5} \tag{19}$$

for the lognormal pdf.

One way to test whether the bivariate pdf is a lognormal or normal pdf is to test the (log)normality of the univariate pdfs for both parameters. However, this procedure does not guarantee that the resulting multivariate pdf is normal or lognormal (Jobsen, 1992). To test the bivariate normality, the squared Mahalanobis distance, m_i^2, which takes into account the variance and covariance structure of the distribution, is calculated for each observed parameter vector and compared with the χ^2 distribution (Jobsen, 1992). The squared Mahalanobis distance m_i^2 between an observation (x_i, y_i) and the sample means $(\bar{x},\bar{y})$ for a bivariate distribution is given by:

$$m_i^2 = (x_i - \bar{x})' S^{-1} (x_i - \bar{x}) \tag{20}$$

where S is the sample covariance matrix containing s_x, s_y and $r_{x,y}$ which are the sample standard deviation of x and y, and the sample correlation between x and y, respectively. The ordered m_i^2-values are compared with the percentiles of the χ^2 distribution and a plot of the $(m_i^2, \chi^2_{(1-\alpha),2})$ points, where $(1-\alpha) = (i-0.5)/n$ and n the number of observations, should be close to a straight line. This test is performed using either the untransformed or the $\log_e$-transformed values.

HORIZONTAL SCALE-DEPENDENCY

Van Weesenbeeck and Kachanoski (1991) stressed the importance to validate if the measured field-scale BTCs obtained by spatially averaging local-scale measured BTCs, are representative for 'true' field-scale BTCs. Their criterium to test this is the horizontal scale-dependency of the spreading in the BTCs. The local BTCs are averaged over a spatial scale K as:

$$C_K(z,t,l) = \frac{1}{K}\sum_{i=0}^{K-1} C(z,t,l+i) \tag{21}$$

where $K = 1,\ldots,L$ (and L the number of measured local-scale BTCs), $l = 1,\ldots,L+1-K$. If $K = 1$, then $C_K(z,t,l)$ equals the local-scale BTC, whereas the field-scale BTC at depth z is obtained for $K = L$. For the average BTC at spatial scale K, the average variance is given as:

$$E_K[Var(z)] = E\left[\int_0^\infty [t - E_K(z,l)]^2 C_K(z,t,l)dt\right] \tag{22}$$

where $E[.]$ is the expectation operator and $E_K(z,l)$ the first time moment, given as:

$$E_K(z,l) = \int_0^\infty tC_K(z,t,l)dt \tag{23}$$

Van Weesenbeeck and Kachanoski (1991) reasoned that if the average variance reaches a maximum value with increasing horizontal spatial scale, the estimate of the field-scale variance should be representative for the 'true' field-scale variance since it is no longer function of the horizontal scale. In fact, they compared the shape of the spatial scale-dependency of the variance with the shape of a semivariogram, with the sill referring to the field-scale variance and the range (i.e., the spatial scale at which $E_K[Var(z)]$ reaches its maximum) the minimal spatial scale

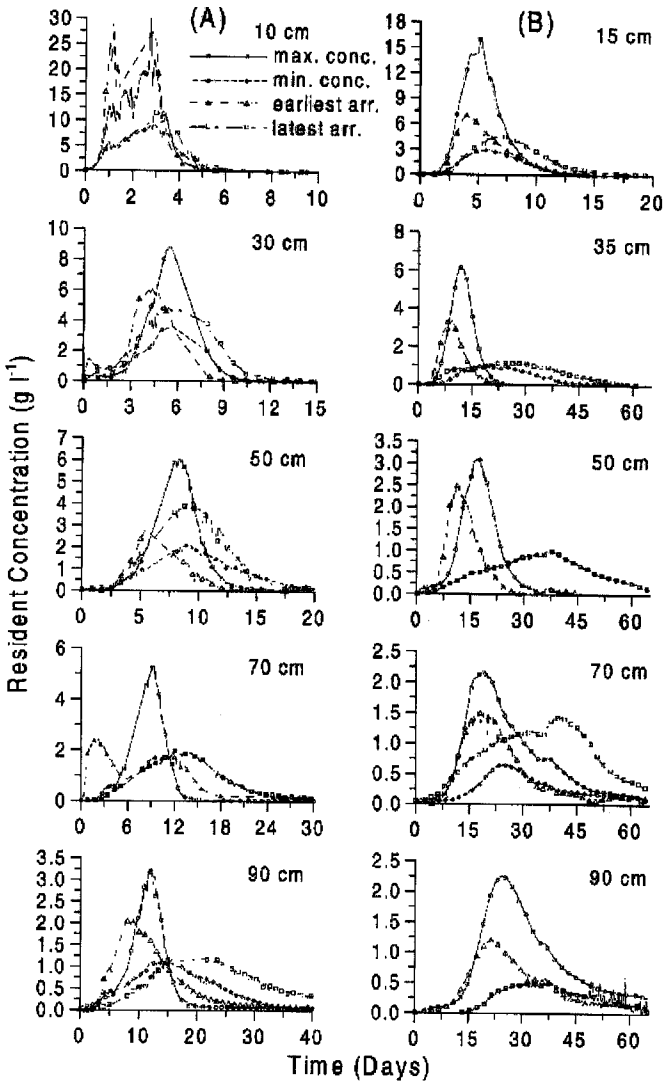

Fig. 2. *Measured extremes for local BTCs at five depths for both fields.*

necessary to obtain reliable estimates of the field-scale BTC (Ward *et al.*, 1994).

Results and Discussion

LOCAL SOLUTE TRANSPORT

The Bekkevoort and Jülich field-sites will be referred to field A and B, respectively. Fig. 2 gives the local resident concentration BTCs for the lowest and highest solute peak, and the earliest and latest BTC in terms of the peak concentration. The extreme BTCs for field A were more irregular, displaying early breakthrough and multiple peaks, whereas those for field B were more uniformly shaped. At the first three depths at field A, most variability between the BTCs was found in the magnitude of the peak concentrations. At the other depths and at field B, the variability in the spread of the BTC is much more pronounced. Except for some extreme BTCs, most BTCs had the typical shape of a CDE or CLT solutions for the transport process.

The CDE- and CLT-model were curve-fitted to all BTCs using an ordinary least-squares optimization, resulting in 120 fitted parameter vectors $\{v,D\}$ for the CDE-model and $\{\mu_l,\sigma_l\}$ for the CLT-model for each site. Some examples of fitted BTCs for both sites are shown in Fig. 3. In general, both models described the observed BTCs fairly well (with R^2 mostly larger than 0.90). In many cases, however, both models underestimate the fast breakthrough, especially at field A. At the first depth in field A (at 10 cm), the CDE and CLT models overestimate the tail of the BTC whereas at larger depths the fitted curves describe the complete BTC quite well.

Determination of the joint multivariate pdf is mostly based on the statistics derived from the univariate parameter pdf. However, the hypothesis of multivariate normality or $\log_e$-normality is rarely checked. The present analysis of the multivariate pdf includes such a check. Fig. 4 shows the differences between the squared Mahalanobis distance m_i^2 and $\chi^2_{(1-\alpha),2}$ plotted against the m_i^2 values based on the original and $\log_e$-transformed parameter vectors for the CDE and CLT models. For field A (Fig. 4a), the distribution of the CDE parameters v and D is better described by the bivariate lognormal pdf because the difference $\{\chi^2_{(1-\alpha),2} - m_i^2\}$ is generally smaller for $\log_e$-transformed than for untransformed parameters. Laboratory solute transport experiments on 30 undisturbed soil columns (20 cm long, 20 cm diameter) taken from the same site in Bekkevoort also revealed lognormally distributed CDE parameters (Mallants *et al*, 1996). The CLT parameters μ_l and σ_l are better described by the bivariate normal pdf (Fig. 4c).

For field B, the CDE and CLT parameters may be described equally well by the bivariate normal as by the bivariate lognormal pdf. The bivariate pdf of v and D was considered lognormal since this is assumed in the CD-STM (Toride and Leij, 1996a). The bivariate pdf of the CLT parameters was assumed to be normal by analogy with the Bekkevoort site. Due to the exponential relation between v, D and μ,σ (Eqns. 9 and 10), a normal distribution of μ and σ involves a lognormal distribution of v and D. Therefore, a normal distribution of μ and σ is in better agreement with the lognormal pdf of v and D reported in other studies (e.g., Biggar and Nielsen, 1976; Van de Pol *et al.*, 1977; Jaynes *et al.*, 1988; Jaynes and Rice, 1993; Gupte *et al.*, 1996; Mallants,1996).

Table 2 summarizes the statistical parameters for the bivariate lognormal pdf for the CDE parameters. For field A, $<v>$ increases with increasing depth due to a larger macroporosity in the topsoil in comparison with the deeper layers. A transport experiment on long undisturbed lysimeters using the same soil under saturated conditions also showed an increase of $<v>$ with depth (Mallants, 1996). It may be that, at shallow depth, the measurement

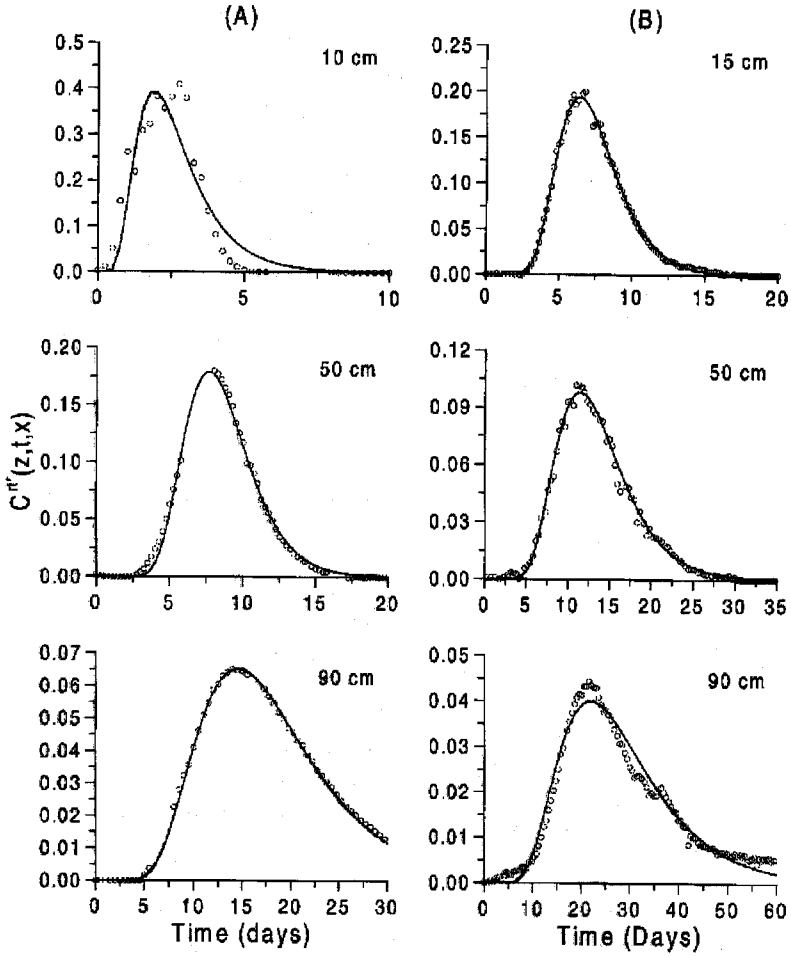

Fig. 3. *Measured BTCs (open circles), fitted CDE- (full line) and CLT-model (dashed line) at three depths for both fields.*

window of the TDR-probes samples mainly the slower transport zones whereas faster transport in macropores is not detected. At greater depths, flow became more homogeneous resulting in a larger transport volume which could be better detected with TDR-probes. Values of $<v>$ for field B were relatively constant with depth suggesting a more similar flow process across horizons. The horizontal variability in v expressed in terms of the coefficient of variation (CV) is somewhat larger in field B then in field A. The largest CVs for field A were found at the deepest depth; the smallest were found at 30 cm. The result was the opposite for field B: the smallest CVs were found at 90 cm, the largest at 35 cm.

The increase of both $<D>$ and the dispersivity $<\lambda> = <D> / <v>$ with depth at both sites contradicts the assumption that the local-scale transport parameters are constant with depth. CV values for D are larger than those for v for both fields. This higher CV of D is in agreement with a higher variability in solute dispersion in comparison with the variability in the occurence of the time of the peak concentration observed at most depths (Fig. 2). Correlation coefficients between v and D were calculated based on their $\log_e$-transforms. Only one such correlation coefficient for field A and three correlation coefficients for field B differ significantly from zero at a significance level of 5% (Table 2).

In Table 3, the statistics of the CLT parameters are given together with the estimated average solute particle velocity based on μ and σ (Eqns 9 and 10). Values for $<v>$, calculated from μ_1 and σ_1, show the same tendency as $<v>$ obtained from the CDE-model, i.e., an increase with depth at field A and relatively constant with depth at field B. At both sites, $<v>$ obtained from the CLT-model is larger than $<v>$ from the CDE-model. This is a consequence of the derivation of $<v>$ from time series of resident concentrations as was shown in the theoretical analyses in, e.g., Jacques *et al.* (1996) and Vanderborght *et al.* (1996).

MACROSCOPIC CDE, VARIANCE AND HORIZONTAL SCALE-DEPENDENCY

In Fig. 5, the observed field-scale BTCs together with the fitted macroscopic CDE are shown. The estimated field-

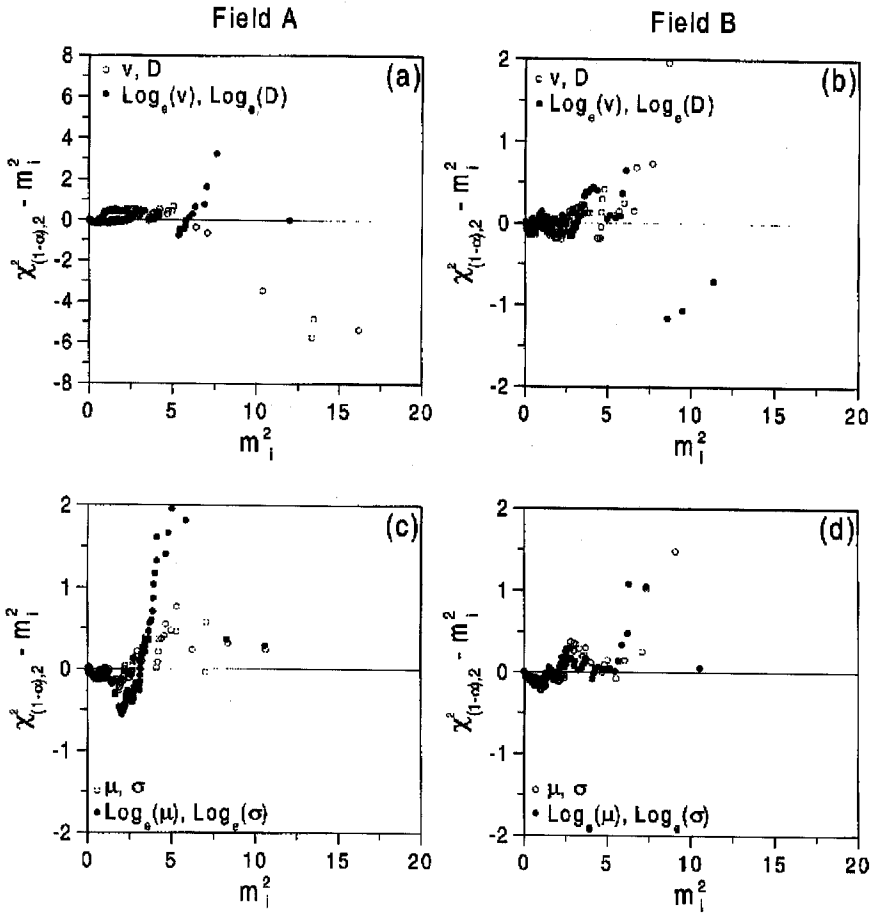

Fig. 4. *The squared Mahalanobis distance, m_i^2, against $\{\chi^2_{(1-\alpha),2} - m_i^2\}$ for original (open circles) and $\log_e$-transformed (closed circles) local transport parameters of the CDE-model (a,b) and the CLT-model (c,d) for field A and B.*

scale parameters $\bar{v}$ and $\bar{D}$ are given in Table 2. For field A, the description of the BTC at early times is not so good throughout the entire soil profile (Fig. 5a). The macroscopic CDE describes the observed field-scale BTC well near the surface of field B (Fig. 5b), but deeper in the soil the leading edge of the BTC is underestimated.

The ensemble mean solute particle velocity, $<v>$, based on the lognormally distributed v parameters of the local-scale BTCs, is generally in agreement with the macroscopic solute velocity, $\bar{v}$ (Table 2). Small differences exist between the ensemble mean dispersion coefficient, $<D>$, and the field-scale dispersion coefficient, $\bar{D}$, for field A. This suggests that the contribution from local velocity fluctuations to field-scale spreading is minimal in field A. Values for $\bar{D}$ in field B are slightly larger than values for $<D>$, indicating modest contributions from velocity fluctuations to field-scale dispersion. Similar observations were made for the CLT parameters: the $<\mu>$ and $<v>$ are at some depths larger and at other depths smaller than the $\bar{\mu}$ and $\bar{v}$ of the field-averaged BTC (Table 3). Also $\bar{\sigma}$ of the field-averaged BTC is larger than $<\sigma>$, and the difference between $<\sigma>$ and $\bar{\sigma}$ is small for field A and moderate for field B. Schulin *et al.* (1987) also found that the ensemble averages of the local velocities agreed well with the macroscopic solute velocity, but that differences between averaged local dispersivities and field-scale dispersivity were rather large. In the study of Gupte *et al.* (1996), similar small differences between field-scale parameters and the ensemble averages of local-scale parameters as in the present study were found. With respect to stochastic simulations using a STM, Gupte *et al.* (1996) showed that deterministic CDE predictions of the field-scale BTC, based on $<v>$ and $<D>$, were in good agreement with stochastic predictions based on the CD-STM. In contrast, Destouni *et al.* (1994) found a large discrepancy between the arithmetic averages of the local-scale and the field-scale transport parameters. They concluded that the statistics of solute transport parameters should be estimated for the scale of interest. These different conclusions can be explained by the imposed boundary condition. If solute transport is measured under ponding conditions, large differences between local and field-scale λ were found (Destouni *et al.*, 1994; Mallants, 1996). Without ponding, local-scale λ was close to the field-scale λ and a deterministic approach may be adequate (Gupte *et al.*, 1996).

The dispersivity of field A is much smaller than the

observed λ in the lysimeter study of Mallants (1996) where solute transport was measured using TDR-probes under ponding conditions in 14 undisturbed soil columns (1 m high, 30 cm diameter) containing the same soil. For example, Mallants (1996) observed a dispersivity of 65 cm at 90 cm depth, whereas λ is only 6.14 cm in this study (Table 2). Jaynes *et al.* (1988) also reported that the field-scale λ measured under flooded irrigation was larger than the field-scale λ under intermittent irrigation. The larger λ under ponding conditions is probable due to solute transport through macropores and to a larger variability in saturated hydraulic conductivity than the variability of the unsaturated conductivity (e.g., Mohanty *et al.*, 1996).

Also shown in Fig. 5 (right) is the observed variance of the measured resident concentration in the horizontal direction. A double peak behaviour is observed at several depths in the two fields (at 10, 30 and 70 cm at field A, and 15 and 90 cm at field B) as was also observed in the numerical studies of Burr *et al.* (1994) and Harter and Yeh (1996) and the experimental study of Mallants (1996). Similar to other studies (Burr *et al.*, 1994; Toride and Leij, 1996b; Mallants, 1996), the minimum of the variance coincidences with the time of the peak concentration, e.g., at the fifth depth in field B. The CV of the resident concentration is minimal around the peak concentration and maximal in the two outer parts of the BTCs which is in agreement with the other studies. For example, the CV at the peak concentration is around 20% for field A and between 38% and 50% at field B. In contrast, CV-values of the BTC at early times reach a maximum of 300% for

Table 2. Statistics of the CDE parameters from the CDE-model and observed effective parameter.

Field A						
Depth	(cm)	10	30	50	70	90
N*		24	24	23	24	23
θ	($cm^3\ cm^{-3}$)	0.370	0.346	0.350	0.354	0.356
$<v>^{++}$	($cm\ day^{-1}$)	4.930^A	5.605^B	6.496^C	7.100^C	6.653^C
σ_{lnv}		0.110	0.072	0.092	0.123	0.175
CV_v^{**}		11.03	7.21	9.12	11.03	17.53
$<D>^{++}$	($cm^2\ day^{-1}$)	6.716^A	7.950^A	13.802^B	24.007^C	40.879^D
σ_{lnD}		0.320	0.326	0.379	0.439	0.565
CV_D^{**}		33.92	33.49	39.49	46.10	61.32
λ	(cm)	1.133	1.418	2.125	3.381	6.144
ρ_{vD}		0.716^+	0.109	0.093	0.000	0.117
$\bar{v}^{***}$	($cm\ day^{-1}$)	4.14	5.40	6.34	7.04	6.64
D^{***}	($cm^2\ day^{-1}$)	5.91	7.00	12.44	26.35	42.41
Field B						
Depth	(cm)	15	35	50	70	90
N*		19	21	22	20	20
θ	($cm^3\ cm^{-3}$)	0.376	0.406	0.467	0.452	0.430
$<v>^{++}$	($cm\ day^{-1}$)	2.540^A	2.673^A	2.675^A	2.417^A	2.508^A
σ_{lnv}		0.174	0.276	0.227	0.151	0.145
CV_v^{**}		17.53	28.13	23.00	15.19	14.58
$<D>^{++}$	($cm^2\ day^{-1}$)	2.824^A	5.966^B	8.844^B	13.552^C	14.109^D
σ_{lnD}		0.413	0.290	0.334	0.295	0.407
CV_D^{**}		43.13	29.62	34.35	30.15	42.45
λ	(cm)	1.112	2.234	3.308	5.607	5.626
ρ_{vD}		0.714^+	0.155	0.135	0.474^+	0.745^+
$\bar{v}^{***}$	($cm\ day^{-1}$)	2.47	2.73	2.68	2.40	2.44
D^{***}	($cm^2\ day^{-1}$)	3.32	7.68	11.02	17.49	16.32

* number of BTCs analyzed
** coefficient of variation
*** estimated parameters to the observed field-scale BTC
$^+$ significant different from 0 at significancy level of 5 %.
$^{++}$ Depths with different letters have significant different means of the local parameter

Table 3. Statistics of the CLT parameters obtained by ordinary least squares optimization (same units as Table 2).

			Field A		
Depth	10	30	50	70	90
$<\mu_l>^+$	2.833[A]	2.795[A]	2.663[B]	2.582[B]	2.604[B]
CV_μ	5.06	2.54	3.45	4.49	6.78
$<\sigma_l>^+$	0.511[A]	0.297[B]	0.281[B]	0.300	0.344[B]
CV_σ	10.72	15.91	18.14	21.25	25.72
<v>	4.941	5.857	6.721	7.270	7.050
σ_{lnv}	0.123	0.070	0.091	0.118	0.166
CV_V	12.39	7.01	9.15	11.83	11.47
<D>	7.682	8.345	14.425	25.238	43.921
CV_D	35.15	34.95	40.86	47.87	64.16
$\bar{\mu}^{**}$	2.95	2.84	2.68	2.55	2.58
$\bar{\sigma}^{**}$	0.50	0.29	0.28	0.32	0.36
μ_{eff}^*	2.87 (2.87)	2.79 (2.79)	2.65 (2.66)	2.57 (2.58)	2.57 (2.59)
σ_{eff}^*	0.53 (0.51)	0.31 (0.30)	0.30 (0.28)	0.32 (0.30)	0.39 (0.34)
			Field B		
Depth	15	35	50	70	90
$<\mu l>^+$	3.552[A]	3.536[A]	3.522[A]	3.589[A]	3.584[A]
CV_μ	5.28	7.00	5.87	4.258	4.55
$<\sigma_l>^+$	0.369[A]	0.350[A]	0.352[A]	0.382[A]	0.334[A]
CV_σ	10.18	18.54	18.11	11.92	14.63
<v>	2.719	2.830	2.836	2.594	2.653
σ_{lnv}	0.180	0.263	0.217	0.151	0.153
CV_V	18.16	26.78	21.97	15.18	15.40
<D>	3.090	6.337	9.429	14.569	14.936
CV_D	36.52	31.06	36.07	31.52	44.00
$\bar{\mu}^{**}$	3.54	3.46	3.47	3.55	3.58
$\bar{\sigma}^{**}$	0.41	0.39	0.39	0.44	0.37
μ_{eff}^*	3.51 (3.54)	3.44 (3.51)	3.45 (3.50)	3.56 (3.58)	3.55 (3.58)
σ_{eff}^*	0.41 (0.37)	0.44 (0.35)	0.41 (0.35)	0.41 (0.38)	0.37 (0.33)

* $\sigma^2_{lnv} \neq 0$ ($\sigma^2_{lnv} = 0$)
** estimated parameters to the observed field-scale BTC
\+ Depths with different letters have significant different means of the local parameter

both fields, whereas CV-values of the tailing part have maximum values of 100% at field A and 500% at field B.

The horizontal scale-dependency of the spreading in the BTC expressed as the time variance (Eqn. (22) was investigated using the approach of van Weesenbeeck and Kachanoski (1991)). The results are presented in Fig. 6. For the first three depths in field A, there is almost no spatial range, indicating that almost all solute transport heterogeneity at the field-scale is captured within a single TDR-measurement volume. Deeper in the soil, however, solute transport shows heterogeneity at a larger scale, probably due to the redistribution of water flow. This is also clear in Fig 2a, where the variability of the time of peak concentration increases with depth. The redistribution may result in the formation of stream paths having different water fluxes along the transect. Numerical simulations of water and solute flow in heterogeneous soil indicate that even for a homogeneous flow rate at the input surface, water flow is funnelled in stream paths close to the input surface (e.g., Roth, 1995; Fig. 1 in Harter and Yeh, (1996); Vanderborght *et al.*, 1997b). Another feature of the curves at field A is the decrease of E[var(t)] at a spatial scale of 6 meter, probably because the influence of extreme local BTCs is smaller if they are averaged over a larger scale.

An increasing range of the scale-dependency and an increasing difference between the local-scale and the field-scale E[Var(t)] with depth is also observed at field B (Fig. 6b). At the second, and to a lesser extent at the third depth, a sharp increase in the E[var(t)] is observed followed by a decrease. This is the effect of one local BTC with high solute dispersion (Fig. 2b) resulting in a large

time variance. However, if the average is taken over several adjacent BTCs, the influence of the solute dispersion on E[var(t)] is smoothed. At the fifth depth, two sill values are observed, one with a range of about 1 m and the other with a range of 4 m. In other words, three different scales of heterogeneity are observed: (1) the heterogeneity captured within the TDR-measurement volume, (2) the heterogeneity acting at a spatial scale between 1 and 2 m, and (3) the heterogeneity acting at a scale larger than 4 m. The first scale can be explained by the existence of local stream tubes with different pore water velocities within the TDR-measurement volume (see Fig. 1b and 1c). The second scale can be related to the formation of the stream paths, since a range of 1 m is also observed at the third and fourth depth. The last scale is probably related to changing soil properties caused by some underlying factors, similar to nested variograms (Goovaerts, 1992). The only indication for changing soil properties is a higher water content in the second half of the transect at this depth (Jacques *et al.*, 1996). However, no reason is found why the water content increases along the transect.

This study of the scale-dependency of the time variance of resident concentrations indicates that the measured field-averaged BTC is representative of the 'true' field-scale BTC since the curves reach a sill value at a spatial scale smaller that 8 m. In addition, it shows that *in-situ* water flow and solute transport processes exhibit a large variability, even at a small scale. This was also observed in many other studies (e.g., Schulin *et al.*, 1987; Jensen and Refsgaard, 1991).

FIELD-SCALE TRANSPORT

Thus far, the effective field-scale parameters of the CDE- and CLT-models have been compared with the ensemble averages of the local-scale CDE- and CLT-parameters. In this final section, the arithmetic average of the measured BTCs (estimate of the effective field-scale transport) will be compared with those predicted by the three different STM models. The following discussion will focus on (i) the relative importance of the local-scale transport heterogeneity, and how to represent it, and on (ii) the validation of the three STMs.

(1) Stochastic Piston Flow STM

The importance of solute transport heterogeneity is investigated using the stochastic piston flow STM with only the pdf of the local v as input. Three different estimates of the solute particle velocity were used, namely (i) the piston flow average solute particle velocity, v_p ($= j_w/\theta$), with j_w the applied water flux and θ the measured water content, (ii) v_{CDE} obtained from Eqn. (7), and (iii) calculated values for v_{CLT} using Eqn. (9).

The predictions for field B based on the pdfs for v_{CDE} and v_{CLT} are shown in Fig. 7. Similar results were obtained for field A (not shown here). It is clear that describing a local-scale transport process by a piston flow model will lead to an overprediction of the peak concentration and an underestimation of the field-scale dispersion. Estimates of D_{eff}, based on the statistics of the pdf of v_{CDE} and v_{CLT} (Table 1), are approximately 4 times smaller than D obtained from fitting the macroscopic CDE (Eqn. (6)) to the field-scale BTC at 90 cm depth. The underestimation of the field-scale dispersion is even more pronounced if v_p is used, since the CV of v_p (= 2.7 %) is smaller than the CV of v_{CDE} (= 14%) and of v_{CLT} (= 15%). At 90 cm depth, D_{eff} based on v_p is 10 times smaller than D. Since the CV of v_p is much smaller than the CV of the average solute particle velocity, v_{CDE}, the observed variability of v_{CDE} cannot be explained by the CV of the observed water content θ.

Neglecting local heterogeneity or dispersion of solute transport within the measurement volume of the TDR probe leads to a severe underestimation of the field-scale solute dispersion. In other words, the dispersion of the field-scale BTC is the result of solute spreading processes acting at different scales, i.e., the solute spreading at the local scale and an additional spreading mechanism at the field-scale due to variability in local v. This is confirmed by the results from the scale- dependency analysis. Since the difference between D and the predicted D_{eff} based on the stochastic piston flow model is quite large, local-scale transport heterogeneity contributes significantly to the field-scale dispersion process. These results agree with the lysimeter study of Poletika *et al.* (1995), which revealed that 73% of the total variance of the mean BTC was attributed to the solute spreading process at the local-scale. The significant contribution of the local-scale spreading process is also demonstrated in the study of Gupte *et al.* (1996).

(2) Convective-Dispersive Stream Tube Model (CD-STM)

The statistics (μ_v, μ_D, σ_v, σ_D and ρ_{vD}) of the local-scale CDE parameters (Table 2) were used to predict the field-scale solute BTC using Eqn. (1). Fig. 5 shows the mean measured and predicted BTCs for field A and B using one set of parameters calibrated for each depth. For both fields, there is a good agreement between measurements and predictions, except at the first depth for field A. Deterministic predictions, using $<v>$ and $<D>$, were also performed (results not shown). These deterministic predictions were in close agreement with the stochastic predictions for field A confirming the earlier statement that velocity fluctuations contribute minimally to field-scale dispersion. Deterministic predictions for field B were slightly different from the stochastic predictions (higher peak concentrations, smaller solute dispersion). Predictions of the variance (Fig. 5) using the STM vary from good to reasonably good. However, the predictions of the variance are much better than the simulations reported by Mallants (1996).

The original five parameter STM can be simplified assuming (i) a constant dispersivity, $\lambda = <D>/<v>$ for the

entire field (v and D are perfectly positive correlated and $\sigma_D = \sigma_v$, see Eqn. (2.2) in Toride and Leij, 1996b), or (ii) a deterministic dispersion coefficient $<D>$ ($\sigma_D = 0$). Predictions with those assumptions for the 90 cm depth are shown in Fig. 8. It is clear that the influence of the variability of the local D on the field-scale solute BTC is of minor importance, although the assumptions for (i) and (ii) are in disagreement with the data given in Table 2. The same conclusions were derived from the comparison of the different effective CDE estimates and for the other depths. These observations are in agreement with the studies of Bresler and Dagan (1981), Amoozegard-Fard *et al.* (1982), Toride and Leij (1996a), and the lysimeter study of Mallants (1996).

As could be expected, the CD-STM accurately describes the field-scale BTC at the same depth of the determination of the local solute transport parameters. It is also important to investigate how good this STM can predict the solute breakthrough at other depths in order to have an independent validation of the STM. For field A, we used the statistics of 30 cm depth, since the field-scale BTC at 10 cm could not be accurately described by both

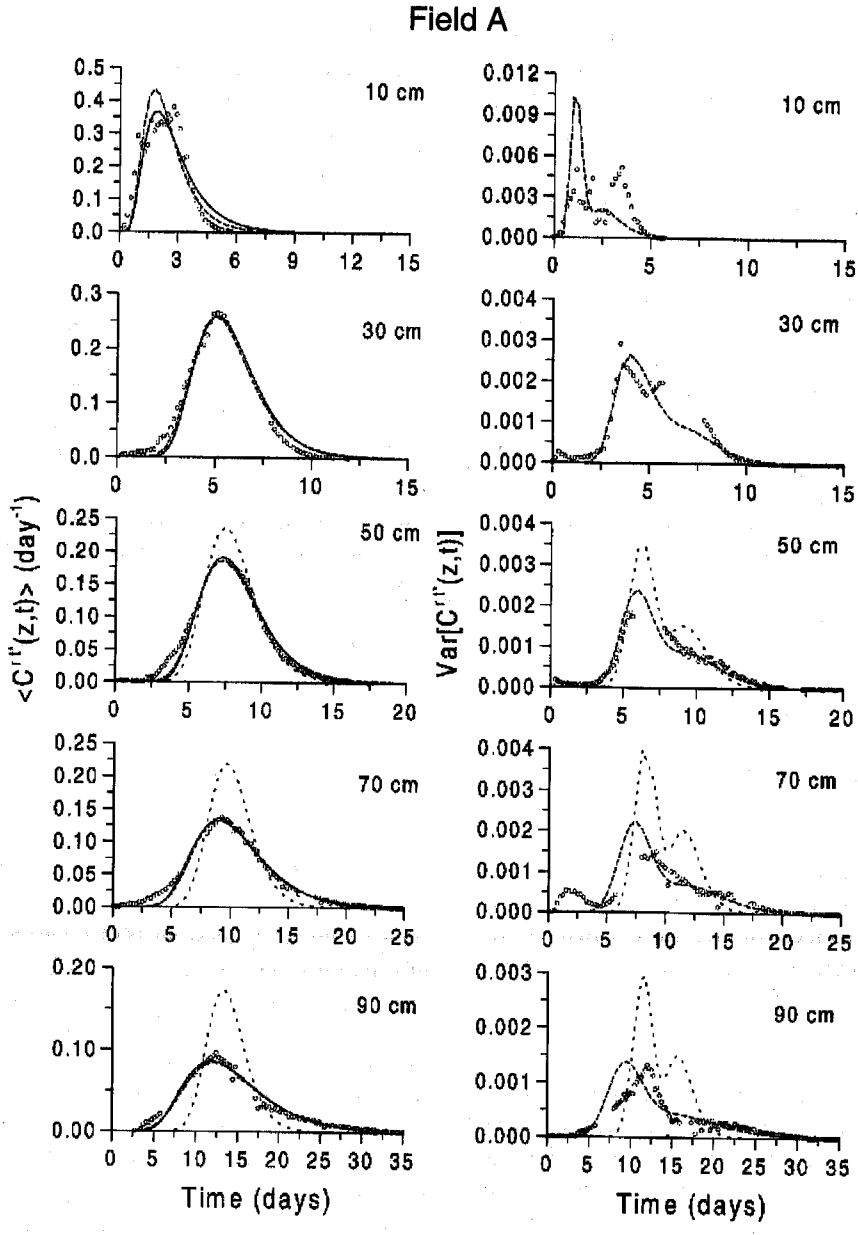

Fig. 5a. (and opposite) *Left: Observed (open circles) field-scale BTCs for field A (fig. 5a) and B (fig. 5b) at the five depths, together with the fitted macroscopic CDE (full line) and predicted field-scale BTCs using the CD-STM (long dashes: predictions with depth dependent parameters, short dashes: predictions with one set of parameters).*
Right: Observed (open circles) variance of the horizontal local resident concentrations for field A (fig. 5a) and B (fig. 5b) at the five depths, together with the predicted variances using the CD-STM (long dashes: predictions with depth dependent parameters, short dashes: predictions with one set of parameters).

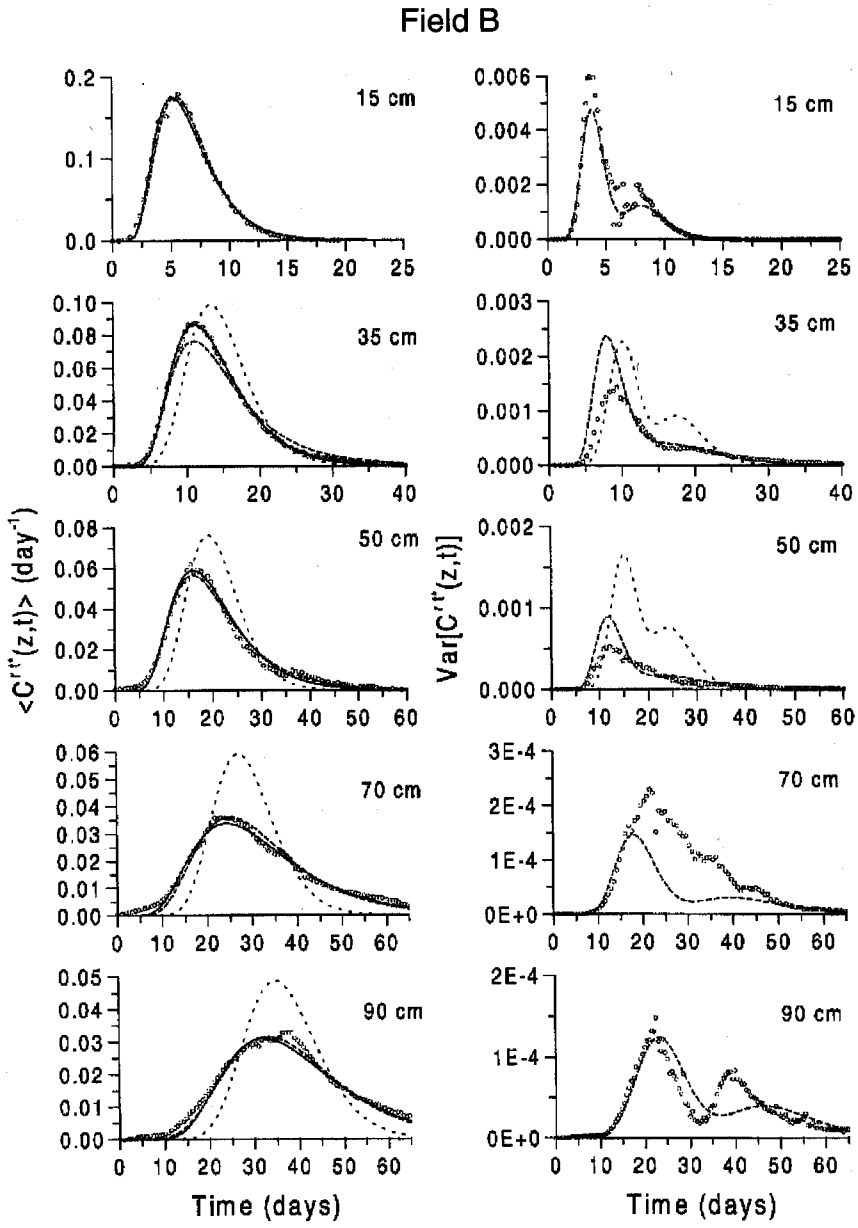

Fig. 5b.

the macroscopic CDE and the STM. Furthermore, the $\langle v \rangle$ was adjusted for each depth according to the values in Table 2, since $\langle v \rangle$ changes with depth. For field B, statistics of the 15 cm depth were used and $\langle v \rangle$ was not adjusted with depth. The predictions (Fig. 5) demonstrate the increasing overestimation of the peak concentration and underestimation of the solute dispersion with depth. Furthermore, the variance in the beginning and the tailing of the breakthrough is underestimated, whereas the maximum observed variance is severely overestimated (the estimated variance at 70 and 90 cm depth for field B is not displayed, since the values were too high). Thus, the assumption that the local transport process, measured with TDR probes, can be described with a local CDE with constant parameters v and D with depth is not fulfilled for these two field experiments. Especially $\langle D \rangle$ increases with depth which is in contradiction with the assumption of a local CDE process (Fig. 1b).

(3) Stochastic-convective lognormal stream tube model (SC-STM)

The predicted field-scale BTCs based on Eqn. (8) using effective parameters μ_{eff} and σ_{eff} (Eqns 11 and 12) for each depth are displayed in Fig. 9. Similar to the CD-STM, the SC-STM model predicts the observed field-scale BTCs very well. Predictions of the variance are obtained using a Monte-Carlo simulation where μ_l is treated as a normally distributed random variable. These estimations display a bimodal behaviour and are relatively close to the observed variance. Estimates of μ_{eff} and σ_{eff} are given in Table 3. In general, μ_{eff} and σ_{eff} are close to the observed $\bar{\mu}$ and $\bar{\sigma}$. This means that the observed CVs of 10–25% of the local σ-parameter, which is in contradiction with the assumption of a deterministic σ, did not influence the predictions of this model. If $\sigma_{lnv} = 0$ in Eqns (11) and (12), predicted field-scale BTCs are little different from the prediction

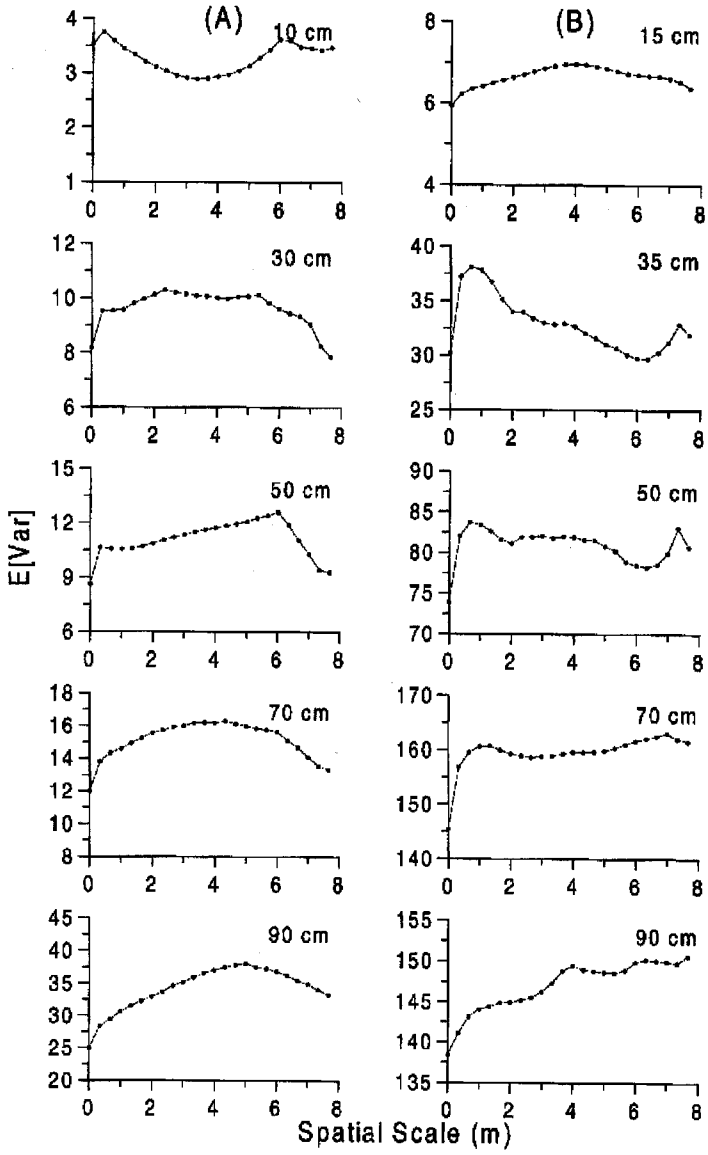

Fig. 6. *Scale-dependency of the time variance for the five depths for (a) field A, and (b) field B.*

with the observed $\sigma_{\ln v}$ (results not shown) and also μ_{eff} and σ_{eff} are close to the observed ones (Table 3). This illustrates again the large contribution of local-scale heterogeneity, characterized by $<\sigma>$, in comparison with the variability of v across the transect.

Similar to the analysis of the CD-STM, the predictions of BTCs at different depths using one set of parameters (30 cm depth for field A, and 15 cm for field B) were compared with the observed BTCs in Fig. 9. An analogue correction for the changing $<\mu_l>$ with depth for field A is done. In contrast to the result from the CD-STM, the SC-STM predicts the peak concentration and the field-scale dispersion accurately for all depths. Variance predictions from either a different set of parameters for each depth, or one set of parameters for all depths, do not differ in their shape but mainly in their magnitude. The difference between the two depends on the relative magnitude of the standard deviation of the local μ_l or $\ln(v)$: if $\sigma_{\ln v}$ at a certain depth z_2 is larger than the $\sigma_{\ln v}$ from another depth z_1, which is used to predict the field-scale BTC at z_2 with the SC-STM, the predicted variance using the parameters of z_1 will be lower than the predictions using the parameters of z_2, and vica versa. Thus, the SC-STM can describe the field-scale BTCs at different depths meaning that the local-scale transport can be represented by the transport processes outlined above (Fig. 1c). Furthermore, small differences of $<\sigma_l>$ and $\sigma_{\ln v}$ between different depths, as the ones observed in this study, have only a minor influence on the predicted field-scale BTC (Fig. 9). However, these parameters have a significant effect on the predicted variance of the local BTCs which is larger for larger $\sigma_{\ln v}$.

Summary and Conclusions

In this study, the transition of scale of a transport process, i.e., from local-scale to a field-scale, was investigated. Predictions of the field-scale transport process were made within a stochastic framework in which the soil is viewed as a set of non-interacting and vertically homogeneous soil columns. Solute movement at the local-scale was described by assuming either a CDE- or a CLT-model. Field-scale solute transport was then predicted based on the statistics of the uni- or bivariate pdfs of the local-scale solute transport parameters. The major conclusions of this study are:

(1) TDR-measured time-series of solute resident concentrations at 5 depths and 24 locations along a 8 m long transect in a loamyy and silty-loam field could be described well by the local CDE- or CLT-model.

(2) Transport parameters v and D for the CDE-model are bivariate lognormally distributed. The parameters μ_l and σ_l for the CLT-model are bivariate normally distributed. This implies that the average solute particle velocity and the dispersion coefficient, calculated as an exponential function of μ_l and σ_l, are lognormally distributed.

(3) The differences between the ensemble averages of the local-scale parameters and the parameters describing the field-scale BTC are small for the loamy soil (field A) and moderate for the lsilty-oam soil (field B). This illustrates that the local-scale solute transport heterogeneity contributes significantly to the total field-scale dispersion. Also, the study of the scale-dependency revealed the importance of small-scale variability, especially near the soil surface. Deeper in the soil, large-scale variability of water fluxes plays a more important role. This process is probably due to the horizontal water redistribution in the soil.

(4) The stochastic piston flow STM overpredicted the mean peak concentrations considerably and underpredicted the solute dispersion illustrating again that the local-scale variability contributes significantly to the field-scale solute dispersion. Both the CD-STM and the SC-

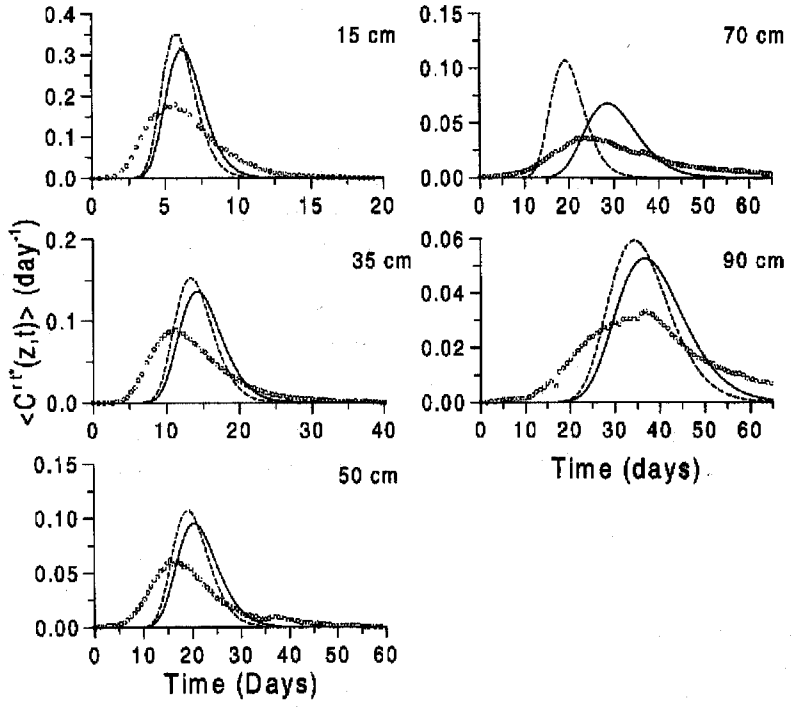

Fig. 7. *Observed (open circles) and predicted field-scale BTCs for field B using the stochastic piston flow STM based on v_{CDE} (full line) and v_{CLT} (dashed line).*

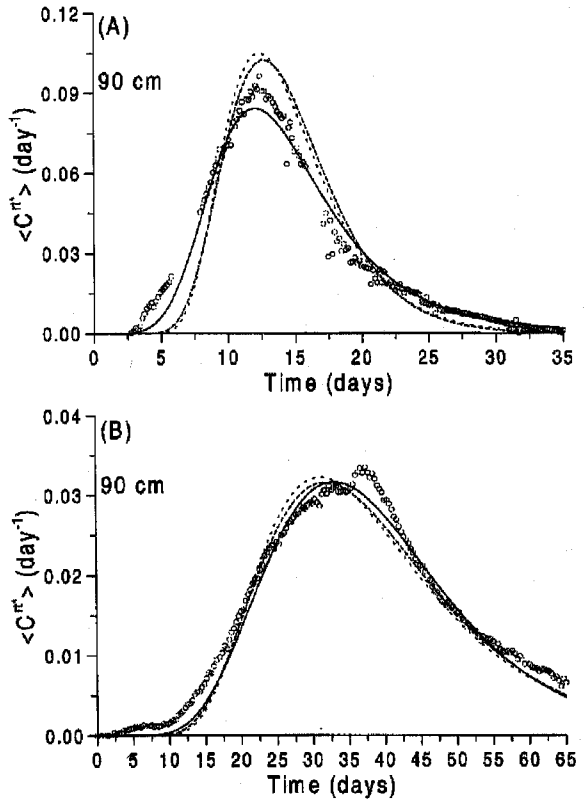

Fig. 8. *Observed (open circles) and predicted (lines) field-scale BTCs at 90 cm depth at (a) field A and (b) field B for fitted parameters (full line), for $\rho_{vD} = 1$ and $\sigma_D = \sigma_v$ (long dashes) and for $\sigma_D = 0$ (short dashes).*

STM generally gave good predictions of the field-scale BTCs and reasonably good descriptions of the variance. However, if only one set of parameters calibrated at shallow depths was used to describe the field-scale BTCs at different depths, the SC-STM was better than the CD-STM. Therefore, the local-scale transport, as measured with TDR-probes, should be viewed as a correlated flow model or a stochastic convective transport process described by the CLT-model.

(5) The predictions with the SC-STM revealed that the field-scale BTC estimates are robust to the small differences of $<\sigma_{\ln}>$ and $\sigma_{\ln v}$ with depth observed in this study. In contrast, estimates of the variance of the local BTCs in the horizontal direction are sensitive to $\sigma_{\ln v}$.

Acknowledgement

This study is part of the research *'Critical parameters governing the mobility and fate of agrochemicals in soil/aquifer systems'* (EV5-CT92–0214) and the research *'Risk analysis of the impact of agrochemicals on soil and water quality under farming systems with different land use practices'* (EV5-CT94–0480) financed by the Environmental Programme of the European Union. The first author acknowledges the financial support of a scholarship of the Flemish Institute for the Encouragement of Scientific-Technological Research in the Industry (IWT). The comments of Thomas Harter to improve the quality of the paper are highly appreciated.

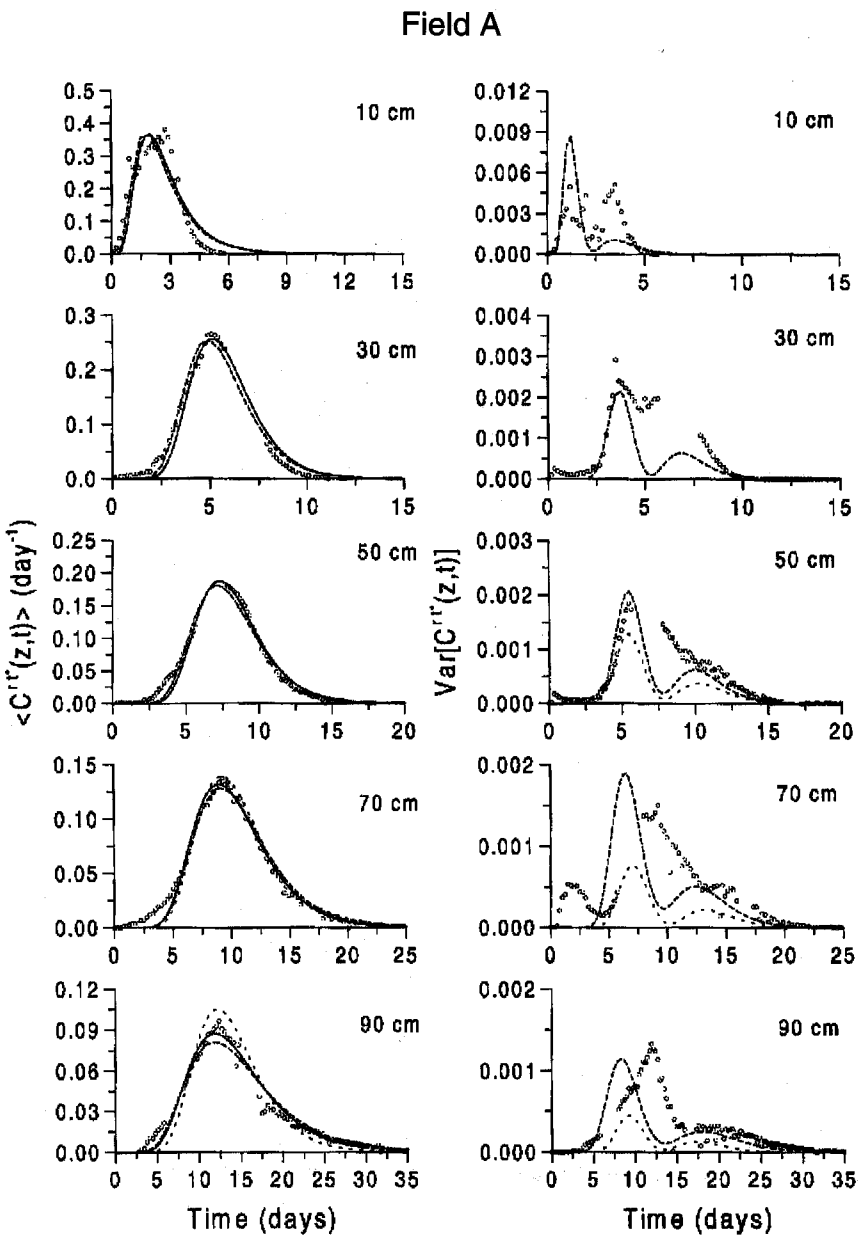

Fig. 9a. (and opposite) *Left: Observed (open circles) field-scale BTCs for field A (fig. 9a) and B (fig. 9b) at the five depths, together with the fitted macroscopic CLT (full line) and predicted field-scale BTCs using the SC-STM (long dashes: predictions with depth dependent parameters, short dashes: predictions with one set of parameters).*
Right: Observed (symbols) variance of the horizontal local resident concentrations for field A (fig. 9a) and B (fig. 9b) at the five depths, together with the predicted variances using the SC-STM (long dashes: predictions with depth dependent parameters, short dashes: predictions with one set of parameters).

References

Aitcheson, J. and Brown, J.A.C. (1963) *The lognormal distribution.* Cambridge University Press, London.

Amoozegar-Fard, D., Nielsen, D.R. and Warrick W.W. (1982) Soil solute concentration distributions for spatially varying pore water velocities and apparent diffusion coefficients. *Soil Sci. Soc. Am. J.* **46**: 3–9.

Beven, K.J., Henderson, D.Ed. and Reeves, A.D. (1993) Dispersion parameters for undisturbed partially saturated soil. *J. Hydrol.* **143**: 19–43.

Biggar, J.W. and Nielsen, D.R. (1976) Spatial variability of the leaching characteristics of a field soil. *Wat. Resour. Res.* **12**: 78–84.

Bowman, R.S. and Rice, R.C. (1986) Transport of conservative tracers in the field under intermittent flood irrigation. *Wat. Resour. Res.* **22**: 1531–1536.

Bresler, E. and Dagan, G. (1979) Solute dispersion in unsatu-

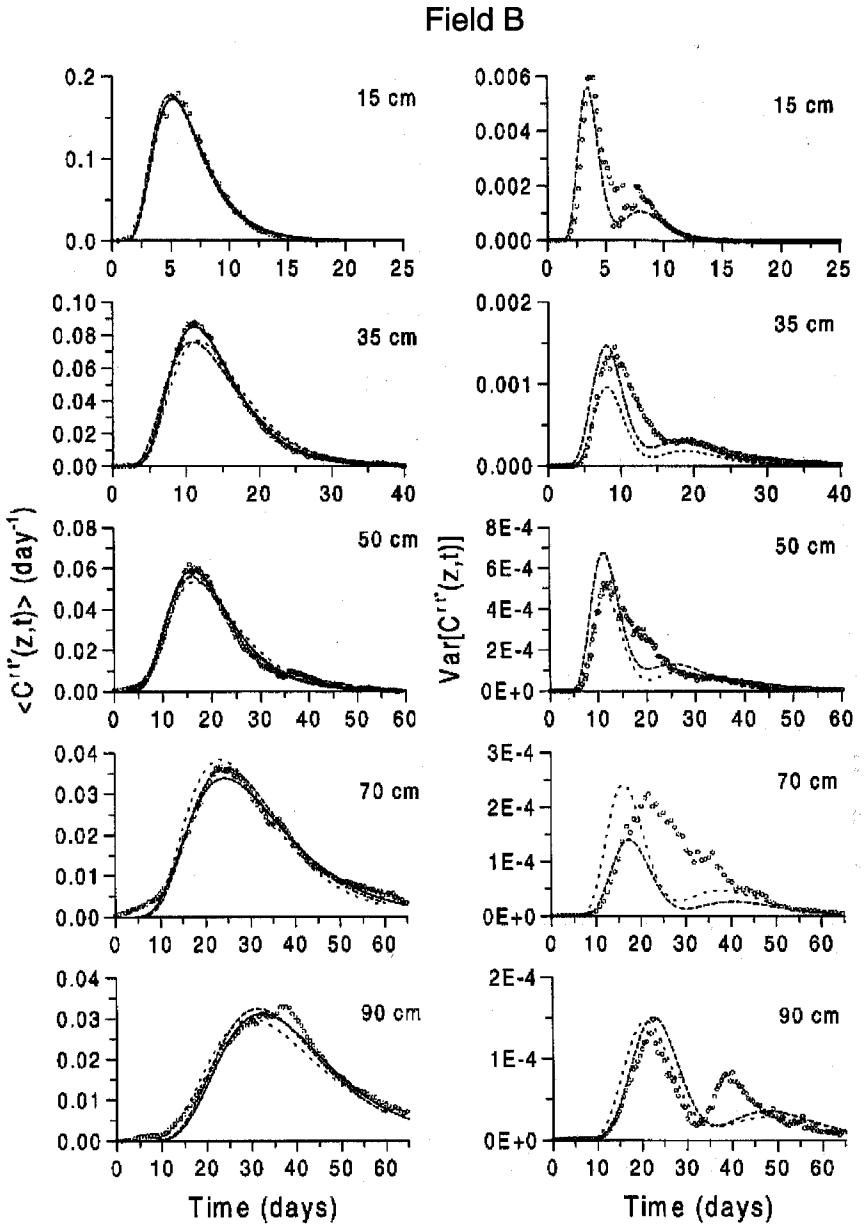

Fig. 9b

rated heterogeneous soil at field-scale: II. Application. *Soil Sci. Soc. Am. J.* **43**: 467–472.

Bresler, E. and Dagan, G. (1981) Convective and pore-scale dispersive solute transport in unsaturated heterogeneous field. *Wat. Resour. Res.* **17**: 1683–1693.

Burr, D.T., Sudicky, E.A. and Naff, R.L. (1994) Nonreactive and reactive solute transport in three-dimensional heterogeneous porous media: Mean displacement, plume spreading, and uncertainty. *Wat. Resour. Res.* **30**: 791–815.

Butters, G.L. and Jury, W.A. (1989) Field scale transport of bromide in an unsaturated soil. 2. Dispersion modelling. *Wat. Resour. Res.* **25**: 1583–1589.

Dagan, G. (1993) The Bresler-Dagan model of flow and transport: Recent theoretical developments. pp. 14–32. In: D. Russo and G. Dagan, eds., *Water flow and solute transport in soils*. Springer-Verlag, Berlin, Heidelberg.

Dagan, G. and Bresler, E. (1979) Solute dispersion in unsaturated heterogeneous soil at field scale: I. Theory. *Soil Sci. Soc. Am. J.* **43**: 461–467.

Destouni, G. (1993) Field-scale solute flux through macroporous soils. pp. 33–34. In: D. Russo and G. Dagan, (eds.), *Water flow and solute transport in soils*. Springer-Verlag, Berlin, Heidelberg.

Destouni, G., Sassner, M. and Jensen, K.H. (1994) Chloride migration in heterogeneous soil, II. Stochastic modelling. *Wat. Resour. Res.* **30**: 747–758.

Ellsworth, T.R., Shouse, P.J., Skaggs, T.H., Jobes, J.A. and Fargerlund, J. (1996) Solute transport in unsaturated soil: Experimental design, parameter estimation, and model discrimination. *Soil Sci. Soc. Am.* J. **60**: 397–407.

Goovaerts, P. (1992) *Multivariate geostatistical tools for studying scale-dependent correlation structures and describing space-time variability*. Thèse, Université Catholique de Louvain.

Gupte, S.M., Radcliffe, D.E., Franklin, D.H., West, L.T., Tollner, E.W. and Hendrix, P.F. (1996) Anion transport in a piedmont ultisol: II. Local-scale parameters. *Soil Sci. Soc. Am. J.* **60**: 762–770.

Hamlen, C.J. and Kachanoski, R.G. (1992). Field study across a soil horizon boundary. *Soil Sci. Soc. Am. J.* **56**: 1716–1720.

Harter, T. and Yeh, T.-C. (1996) Stochastic analysis of solute transport in heterogeneous, variably saturated soils. *Wat. Resour. Res.* **32**: 1585–1595.

Heimovaara, T.J. and de Water, E. (1993) *A computer controlled TDR system for measuring water content and bulk electrical conductivity of soils.* Manual of the automatic TDR system, FGBL, Universiteit of Amsterdam.

Jacques, D., Kim, D.-J., Diels, J., Vanderborght, J., Vereecken, H. and Feyen, J. (1997) Analysis of steady-state chloride transport through two heterogeneous fields. *Wat. Resour. Res.*, submitted.

Jaynes, D.B. and Rice, R.C. (1993) Transport of solutes as affected by irrigation method. *Soil Sci. Soc. Am. J.* **57**: 1348–1353.

Jaynes, D.B., Bowman, R.S. and Rice, R.C. (1988) Transport of a conservative tracer in the field under continuous flood irrigation. *Soil Sci. Soc. Am. J.* **52**: 618–624.

Jensen, K.H. and Refsgaard, J.C. (1991) Spatial variability of physical parameters and processes in two field soils, Part I: Water flow and solute transport at local scale. *Nordic Hydrol.* **22**: 275–302.

Jobsen, J.D. (1992) *Applied Multivariate Data Analysis*, Springer-Verlag, New York, Inc.

Jury, W.A. (1982) Simulation of solute transport using a transfer function model. *Wat. Resour. Res.* **18**: 363–368.

Jury, W.A. (1985) *Spatial variability of soil physical parameters in solute migration: A critical literature review.* EPRI EA–4228 Project 2485–6, Riverside, CA.

Jury, W.A. and Flühler, H. (1992) Transport of chemicals through soils: Mechanism, model, and field applications. *Adv. Agron.* **47**: 141–201.

Jury, W.A. and Roth, K. (1990) *Transfer functions and solute movement through soil*, Birkhauser Verlag Basel.

Jury, W.A. and Sposito, G. (1985). Field calibration and validation of solute transport models for the unsaturated zone. *Soil Sci. Soc. Am. J.* **49**: 1331–1341.

Jury, W.A., Stolzy, L.H. and Shouse, P.H. (1982) A field test of the transfer function model for predicting solute transport. *Wat. Resour. Res.* **18**: 369–375.

Khan, A.U.H. and Jury, W.A. (1990) A laboratory test of the dispersion scale effect in column outflow experiments. *J. Contam. Hydrol.* **5**: 119–132.

Leij, F.J. and Dane, J.H. (1991) Solute transport in a two-layer medium investigated with time moments. *Soil Sci. Soc. Am. J.* **55**: 1529–1535.

Mallants, D. (1996). *Water flow and solute transport in a heterogeneous soil profile.* Ph-D dissertation, K.U.Leuven, 316 p.

Mallants, D., Mohanty, B.P., Vervoort, A. and Feyen, J. (1997a) Spatial analysis of saturated hydraulic conductivity in a soil with macropores. *Soil Technol.* **10**: 115–131.

Mallants, D., Vanclooster, M. and Feyen, J. (1996) Transect study on solute transport in a macroporous soil. *Hydrol. Process.* **10**: 55–70.

Mallants, D., Vanclooster, M., Meddahi, M. and Feyen, J. (1994) Estimating solute transport in undisturbed soil columns using time-domain reflectometry. *J. Contam. Hydrol.* **17**: 91–109.

Mallants, D., Tseng, P.-H., Toride, N., Timmerman, A. and Feyen, J. (1997b) Evaluation of multimodal hydraulic functions in characterizing a heterogeneous field soil. *J. Hydrol.* **195**: 172–199.

Mohanty, B.P., Horton, R. and Ankeny, M.D. (1996) Infiltration and macroporosity under a row crop agricultural field in a glacial till soil. *Soil Sci.* **161**: 205–213.

Poletika, N.N., Jury, W.A. and Yates, M.V. (1995) Transport of bromide, simazine, and MS–2 coliphage in a lysimeter containing undisturbed unsaturated soil. *Wat. Resour. Res.* **31**: 801–810.

Rhoades, J.D., Manteghi, N.A., Shouse, P.J. and Alves, W.J. (1989) Soil electrical conductivity and soil salinity: New formulations and calibrations. *Soil Sci. Soc. Am. J.* **53**: 433–439.

Roth, K. (1995) Steady state flow in an unsaturated, two-dimensional, macroscopically homogeneous Miller-similar medium. *Wat. Resour. Res.* **31**: 2127–2140.

Roth, K. and Hammel, K. (1996) Transport of conservative chemical through an unsaturated two-dimensional Miller-similar medium with steady state flow. *Wat. Resour. Res.* **32**: 1653–1663.

Roth, K., Jury, W.A., Flühler, H. and Attinger, W. (1991) Transport of chloride through an unsaturated field soil. *Wat. Resour. Res.* **27**: 2533–2541.

Rudolph, D.L., Kachanoski, R.G., Celia, M.A., Le Blanc, D.R. and Stevens, J.H. (1996) Infiltration and solute transport experiment in unsaturated sand and gravel, Cape Cod, Massachuttes: Experimental design, and overview of results. *Wat. Resour. Res.* **32**: 519–532.

Russo, D. (1993) Analysis of solute transport in partially saturated heterogeneous soils. In: D. Russo and G. Dagan, (eds.), *Water flow and solute transport in soils,* pp 61–81, Springer-Verlag, Berlin, Heidelberg.

SAS Institute Inc., 1989. *SAS/STAT® User's Guide*, Version 6, Fourth Edition, Volume 2, Cary, NC, Sas Institute Inc., 846 pp.

Schulin, R., van Genuchten, M.Th., Flühler, H. and Ferlin, P. (1987) An experimental study of solute transport in a stony field soil. *Wat. Resour. Res.* **22**: 1785–1795.

Simmons, C.S. (1982) A stochastic-convective transport representation of dispersion in one-dimensional porous media systems. *Wat. Resour. Res.* **18**: 1193–1214.

Spiegel, M.R. (1992) *Shaum's outline of theory and problems of probability and statistics*, Schaum's outline series. McGraw-Hill, New York.

Toride, N. and Leij, F.J. (1996a) Convective-dispersive stream tube model for field-scale solute transport: I. Moment analysis. *Soil Sci. Soc. Am. J.* **60**: 342–452.

Toride, N. and Leij, F.J. (1996b) Convective-dispersive stream tube model for field-scale solute transport: II. Examples and calibration. *Soil Sci. Soc. Am. J.* **60**: 352–361.

Toride, N., Leij, F.J. and van Genuchten, M.Th. (1995) *The CXTFIT Code for estimating transport parameters from laboratory or field tracer experiments.* Research Report No. 137, U.S. Salinity Laboratory, Riverside, California, 121 pp.

Tseng, P-H and Jury, W.A. (1994) Comparison of transfer function and deterministic modelling of area-averaged solute transport in a heterogeneous field. *Wat. Resour. Res.* **30**: 2051–2063.

van de Pol, R.M., Wierenga, P.J. and Nielsen, D.R. (1977) Solute movement in a field soil. *Soil Sci. Soc. Am. J.* **41**: 10–13.

Vanderborght, J., Gonzalez, C., Vanclooster, M., Mallants, D. and Feyen, J. (1997a) Effects of soil type and water flux on solute transport. *Soil Sci. Soc. Am. J.* **61**: 372–389.

Vanderborght, J., Jacques, D., Mallants, D., Tseng, P.-H. and Feyen, J. (1997b). Comparison between field measurements and numerical simulation of steady-state solute transport in a

heterogeneous soil profile. *Hydrol. Earth System Sci.* **1** (4) 853–871.

Vanderborght, J., Vanclooster, M., Mallants, D., Diels, J. and Feyen J. (1996) Determining convective lognormal solute transport parameters from resident concentrations, *Soil Sci. Soc. Am. J.* **60**: 1306–1317.

Van Weesenbeeck, I.J. and Kachanoski, R.G. (1991) Spatial scale dependency of in situ solute transport. *Soil Sci. Soc. Am. J.* **55**: 3–7.

Ward, A.L., Kachanoski, R.G., von Bertoldi, A.P. and Elrick, D.E. (1994) Field and undisturbed-column measurements for predicting transport in unsaturated layered soil. *Soil Sci. Soc. Am. J.* **59**: 52–59.

Zhang, R. (1995) Prediction of solute transport using a transfer function model and the convection-dispersion equation. *Soil Sci.* **160**: 18–27.